

World Journal of *Stem Cells*

World J Stem Cells 2024 June 26; 16(6): 615-738



EDITORIAL

- 615 Searching for the optimal precondition procedure for mesenchymal stem/stromal cell treatment: Facts and perspectives
Zhao YD, Huang YC, Li WS
- 619 Gut microbiota modulating intestinal stem cell differentiation
He L, Zhu C, Zhou XF, Zeng SE, Zhang L, Li K
- 623 Priming mesenchymal stem cells to develop “super stem cells”
Haider KH

ORIGINAL ARTICLE**Clinical Trials Study**

- 641 Safety and efficiency of Wharton’s Jelly-derived mesenchymal stem cell administration in patients with traumatic brain injury: First results of a phase I study
Kabatas S, Civelek E, Boyalı O, Sezen GB, Ozdemir O, Bahar-Ozdemir Y, Kaplan N, Savrunlu EC, Karaöz E

Basic Study

- 656 RPLP0/TBP are the most stable reference genes for human dental pulp stem cells under osteogenic differentiation
Ferreira DB, Gasparoni LM, Bronzeri CF, Paiva KBS
- 670 Mesenchymal stem cells-extracellular vesicles alleviate pulmonary fibrosis by regulating immunomodulators
Gao Y, Liu MF, Li Y, Liu X, Cao YJ, Long QF, Yu J, Li JY
- 690 Outcomes of combined mitochondria and mesenchymal stem cells-derived exosome therapy in rat acute respiratory distress syndrome and sepsis
Lin KC, Fang WF, Yeh JN, Chiang JY, Chiang HJ, Shao PL, Sung PH, Yip HK
- 708 Exosomes from umbilical cord mesenchymal stromal cells promote the collagen production of fibroblasts from pelvic organ prolapse
Xu LM, Yu XX, Zhang N, Chen YS
- 728 Umbilical cord mesenchymal stem cell exosomes alleviate necrotizing enterocolitis in neonatal mice by regulating intestinal epithelial cells autophagy
Zhu L, He L, Duan W, Yang B, Li N

ABOUT COVER

Editorial Board Member of *World Journal of Stem Cells*, Tong Ming Liu, PhD, Senior Research Scientist, Cell Biology and Therapies, Institute of Molecular and Cell Biology, Singapore 138673, Singapore. dbsliutm@yahoo.com

AIMS AND SCOPE

The primary aim of *World Journal of Stem Cells (WJSC, World J Stem Cells)* is to provide scholars and readers from various fields of stem cells with a platform to publish high-quality basic and clinical research articles and communicate their research findings online. *WJSC* publishes articles reporting research results obtained in the field of stem cell biology and regenerative medicine, related to the wide range of stem cells including embryonic stem cells, germline stem cells, tissue-specific stem cells, adult stem cells, mesenchymal stromal cells, induced pluripotent stem cells, embryonal carcinoma stem cells, hemangioblasts, lymphoid progenitor cells, *etc.*

INDEXING/ABSTRACTING

The *WJSC* is now abstracted and indexed in Science Citation Index Expanded (SCIE, also known as SciSearch®), Journal Citation Reports/Science Edition, PubMed, PubMed Central, Scopus, Biological Abstracts, BIOSIS Previews, Reference Citation Analysis, China Science and Technology Journal Database, and Superstar Journals Database. The 2024 Edition of Journal Citation Reports® cites the 2023 journal impact factor (JIF) for *WJSC* as 3.6; JIF without journal self cites: 3.5; 5-year JIF: 4.2; JIF Rank: 16/31 in cell and tissue engineering; JIF Quartile: Q3; and 5-year JIF Quartile: Q3; JIF Rank: 105/205 in cell biology; JIF Quartile: Q3; and 5-year JIF Quartile: Q2. The *WJSC*'s CiteScore for 2023 is 7.8 and Scopus CiteScore rank 2023: Histology is 11/62; Genetics is 78/347; Genetics (clinical) is 19/99; Molecular Biology is 131/410; Cell Biology is 104/285.

RESPONSIBLE EDITORS FOR THIS ISSUE

Production Editor: *Xiang-Di Zhang*; Production Department Director: *Xu Guo*; Cover Editor: *Jia-Ru Fan*.

NAME OF JOURNAL

World Journal of Stem Cells

ISSN

ISSN 1948-0210 (online)

LAUNCH DATE

December 31, 2009

FREQUENCY

Monthly

EDITORS-IN-CHIEF

Shengwen Calvin Li, Carlo Ventura

EDITORIAL BOARD MEMBERS

<https://www.wjgnet.com/1948-0210/editorialboard.htm>

PUBLICATION DATE

June 26, 2024

COPYRIGHT

© 2024 Baishideng Publishing Group Inc

INSTRUCTIONS TO AUTHORS

<https://www.wjgnet.com/bpg/gerinfo/204>

GUIDELINES FOR ETHICS DOCUMENTS

<https://www.wjgnet.com/bpg/GerInfo/287>

GUIDELINES FOR NON-NATIVE SPEAKERS OF ENGLISH

<https://www.wjgnet.com/bpg/gerinfo/240>

PUBLICATION ETHICS

<https://www.wjgnet.com/bpg/GerInfo/288>

PUBLICATION MISCONDUCT

<https://www.wjgnet.com/bpg/gerinfo/208>

ARTICLE PROCESSING CHARGE

<https://www.wjgnet.com/bpg/gerinfo/242>

STEPS FOR SUBMITTING MANUSCRIPTS

<https://www.wjgnet.com/bpg/GerInfo/239>

ONLINE SUBMISSION

<https://www.f6publishing.com>

Basic Study

Exosomes from umbilical cord mesenchymal stromal cells promote the collagen production of fibroblasts from pelvic organ prolapse

Lei-Mei Xu, Xin-Xin Yu, Ning Zhang, Yi-Song Chen

Specialty type: Cell and tissue engineering**Provenance and peer review:** Unsolicited article; Externally peer reviewed.**Peer-review model:** Single blind**Peer-review report's classification****Scientific Quality:** Grade A, Grade B**Novelty:** Grade A**Creativity or Innovation:** Grade A**Scientific Significance:** Grade A**P-Reviewer:** Mohammadi S, Oman**Received:** January 23, 2024**Revised:** March 23, 2024**Accepted:** April 22, 2024**Published online:** June 26, 2024**Processing time:** 153 Days and 20.1 Hours**Lei-Mei Xu, Xin-Xin Yu, Ning Zhang, Yi-Song Chen**, Department of Gynecology, Obstetrics and Gynecology Hospital of Fudan University, Shanghai 200011, China**Lei-Mei Xu**, Department of Gynecology, Shanghai Key Laboratory of Female Reproductive Endocrine-related Diseases, Shanghai 200011, China**Corresponding author:** Yi-Song Chen, Doctor, Chief Doctor, Department of Gynecology, Obstetrics and Gynecology Hospital of Fudan University, No. 128 Shenyang Road, Shanghai 200011, China. cys373900207@163.com

Abstract

BACKGROUND

Pelvic organ prolapse (POP) involves pelvic organ herniation into the vagina due to pelvic floor tissue laxity, and vaginal structure is an essential factor. In POP, the vaginal walls exhibit abnormal collagen distribution and decreased fibroblast levels and functions. The intricate etiology of POP and the prohibition of transvaginal meshes in pelvic reconstruction surgery present challenges in targeted therapy development. Human umbilical cord mesenchymal stromal cells (hucMSCs) present limitations, but their exosomes (hucMSC-Exo) are promising therapeutic tools for promoting fibroblast proliferation and extracellular matrix remodeling.

AIM

To investigate the effects of hucMSC-Exo on the functions of primary vaginal fibroblasts and to elucidate the underlying mechanism involved.

METHODS

Human vaginal wall collagen content was assessed by Masson's trichrome and Sirius blue staining. Gene expression differences in fibroblasts from patients with and without POP were assessed *via* RNA sequencing (RNA-seq). The effects of hucMSC-Exo on fibroblasts were determined *via* functional experiments *in vitro*. RNA-seq data from fibroblasts exposed to hucMSC-Exo and microRNA (miRNA) sequencing data from hucMSC-Exo were jointly analyzed to identify effective molecules.

RESULTS

In POP, the vaginal wall exhibited abnormal collagen distribution and reduced fibroblast 1 quality and quantity. Treatment with 4 or 6 $\mu\text{g}/\text{mL}$ hucMSC-Exo

suppressed inflammation in POP group fibroblasts, stimulated primary fibroblast growth, and elevated collagen I (Col1) production *in vitro*. High-throughput RNA-seq of fibroblasts treated with hucMSC-Exo and miRNA sequencing of hucMSC-Exo revealed that abundant exosomal miRNAs downregulated matrix metalloproteinase 11 (MMP11) expression.

CONCLUSION

HucMSC-Exo normalized the growth and function of primary fibroblasts from patients with POP by promoting cell growth and Col1 expression *in vitro*. Abundant miRNAs in hucMSC-Exo targeted and downregulated MMP11 expression. HucMSC-Exo-based therapy may be ideal for safely and effectively treating POP.

Key Words: Pelvic organ prolapse; Exosomes; Fibroblasts; Human umbilical cord mesenchymal stromal cells; Extracellular matrix; Collagen I

©The Author(s) 2024. Published by Baishideng Publishing Group Inc. All rights reserved.

Core Tip: Our original article, titled “Exosomes derived from hucMSCs promote the growth and collagen production of fibroblasts from pelvic organ prolapse through microRNAs” focused on a promising cell-free treatment for pelvic organ prolapse (POP). Our study the first demonstrated that human umbilical cord mesenchymal stromal cell-derived exosome (hucMSC-Exo) at certain concentrations could facilitate the growth and extracellular matrix remodeling of the primary fibroblasts from POP. Moreover, microRNA sequencing of hucMSC-Exos and high-throughput RNA sequencing of fibroblasts exposed to hucMSC-Exos revealed that highly expressed exosomal microRNAs targeted and downregulated the expression of matrix metalloproteinase 11 in fibroblasts, leading to the increased production of collagen I. These results suggested that hucMSC-Exos could be a promising treatment for POP and may overcome current therapeutic difficulties.

Citation: Xu LM, Yu XX, Zhang N, Chen YS. Exosomes from umbilical cord mesenchymal stromal cells promote the collagen production of fibroblasts from pelvic organ prolapse. *World J Stem Cells* 2024; 16(6): 708-727

URL: <https://www.wjgnet.com/1948-0210/full/v16/i6/708.htm>

DOI: <https://dx.doi.org/10.4252/wjsc.v16.i6.708>

INTRODUCTION

Pelvic organ prolapse (POP) is characterized by the herniation of pelvic organs into the vagina due to laxity of the pelvic supportive system. This disorder not only causes a wide range of physical symptoms, such as vaginal bulging sensation, sexual dysfunction and obstructed defecation but also increases anxiety and decreases self-esteem, thereby imposing heavy social and financial burdens on individuals with POP.

Several studies have reported that prolapsed pelvic tissue is aged and has exhausted collagen fibrils and a decreased quantity and quality of fibroblasts, which results in a diminished ability to support pelvic tissues[1-7]. However, to date, effective therapies for alleviating symptoms and achieving anatomical and functional resolution of POP have not been established. The use of transvaginal polypropylene meshes in prolapse surgery was considered an effective treatment for reducing the anatomic recurrence rate. However, in April, the Food and Drug Administration halted the use of surgical mesh intended for the transvaginal repair of POP due to various severe complications[8-10], such as chronic pain and especially mesh exposure and erosion[11]. Therefore, our effort to develop more effective medical treatments to increase treatment options is warranted to facilitate the restoration of the biological function of fibroblasts from patients with POP.

Recently, mesenchymal stromal cell (MSC)-based therapy was introduced as a promising approach for regenerative medicine due to its powerful functions, such as self-renewal, multipotency and immunoregulatory effects[12]. Among other sources of MSCs, such as bone marrow, adipose tissue, and Wharton’s jelly, human umbilical cord MSCs (hucMSCs) are usually regarded as medical waste and can be obtained without invasive operation or ethical disputes. Thus, hucMSCs can be obtained safely and economically, and they are easy to produce in bulk[13]. Moreover, hucMSCs show great potential to secrete cytokines and have been employed extensively in tissue repair *in vivo* and *in vitro*[14]. Notably, the role of hucMSCs in POP treatment has been investigated. For instance, the use of hucMSC-based bioengineered grafts in sacrocolpexy significantly improved the fiber content and mechanical properties of the vagina in ovariectomized rhesus monkeys[15]. However, various unsolved problems, such as the heterogeneity of progeny stem cells, potential tumorigenesis and immune rejection, limit the application of such grafts[16,17]. In addition, hucMSCs were shown to promote tissue repair and regulate immunity primarily *via* paracrine factors rather than through hucMSC differentiation[12,18]. In our previous study, we constructed an indirect coculture system that allowed the transfer of soluble molecules instead of whole cells. The viability of primary vaginal fibroblasts was increased after coculture with hucMSCs, which indicated that molecules secreted from hucMSCs promoted the growth of primary vaginal fibroblasts from POP[19].

Exosomes (Exos), as one of the main secretory mediators of hucMSCs, have garnered increasing interest as promising cell-free treatments. Exos are nanosized (30-200 nm) cup-shaped extracellular vesicles containing small RNAs and proteins and have bilayer membranes. These vesicles influence numerous biological processes of target cells[20] and lack the risks of cell-based therapies mentioned previously. Several reports have suggested that Exo therapy can reduce mesh exposure and promote the proliferation of capillaries at mesh implantation sites *in vivo*[21,22]. Furthermore, Exos derived from MSCs were reported to induce extracellular matrix synthesis[23,24]. Since Valadi *et al*[25] first reported that microRNAs (miRNAs) within Exos can be transferred to another cell and function at a new site, an increasing number of studies have confirmed that Exo-containing miRNAs have major implications for intercellular communication. Nevertheless, to date, the effects of hucMSC-derived Exos (hucMSC-Exo) on primary pelvic fibroblast function and the underlying mechanisms are still not fully understood.

In this study, we aimed to investigate the effects of hucMSC-Exo on the functions of primary vaginal fibroblasts and to elucidate the underlying mechanism involved. We confirmed the functional relevance of the collected hucMSC-Exo on primary vaginal fibroblasts from different patients with POP. Fibroblasts cocultured with hucMSC-Exo exhibited significantly increased cell viability and collagen I (Col1) production. Mechanistically, high-throughput miRNA sequencing of hucMSC-Exo and RNA sequencing (RNA-seq) of fibroblasts exposed to hucMSC-Exo demonstrated that highly expressed exosomal miRNAs downregulated the expression of matrix metalloproteinase 11 (MMP11) in fibroblasts, contributing to the expansion of Col1. And **Figure 1** is the graphical abstract of our study. Our findings may lead to the development of promising approaches for normalizing the function of fibroblasts in patients with POP.

MATERIALS AND METHODS

Collection of vaginal tissue

After approval from the Obstetrics and Gynecology Hospital of Fudan University (No. 2023-106), full-thickness biopsy samples of the prolapsed anterior vaginal wall (0.5 cm²) were obtained from patients who underwent laparoscopic-assisted vaginal hysterectomy. Informed consent was obtained from all participants. The POP quantitative system[26] was used for grouping: The POP group comprised participants with stages 3 and 4 POP (*n* = 10), and the non-POP group consisted of patients with other benign gynecological diseases, such as hysteromyoma and adenomyosis. No patients had a history of estrogen therapy, pelvic inflammation, serious systemic diseases associated with connective tissue or malignant diseases. No differences in the clinical characteristics between the two groups were found (Table 1). To maintain the consistency and viability of each collected sample, the tissues were separated by surgical scissors without thermal injury and then transferred to the laboratory on ice to isolate fibroblasts aseptically within 20 min.

Histology

Tissue specimens were fixed in 10% buffered formalin and embedded in paraffin. The tissues were cut into 3-5- μ m thick sections and stained with Masson's trichrome and Sirius Red. Collagen deposits were evaluated by brightfield and polarized light microscopy.

Immunohistochemistry

Immunohistochemistry (IHC) was used to evaluate the expression of Col1 in pelvic tissue and vimentin in both the vaginal wall and primary fibroblasts. Paraffin-embedded sections and fixed cells were incubated with primary antibodies (1:500, ab34710, Abcam, United States) overnight at 4 °C, followed by incubation with goat anti-polyvalent biotin-streptavidin (HRP) (RCA054 Thermo Scientific, Waltham, MA, United States).

Primary fibroblast culture

Primary human fibroblasts were aseptically isolated from the vaginal wall following a previously described protocol[27]. The tissues were placed in sterile 100-mm culture dishes and washed 3 times with phosphate-buffered saline (PBS) (Cat. no. B320KJ; Basal Media, China) containing 1% penicillin-streptomycin-amphotericin B agent (Cat. no. C125C8; New Cell & Molecular Biotech, China). Next, the tissues were cut into small pieces and digested in Dulbecco's modified Eagle's medium (DMEM) (Cat. no. B320KJ, Basal Media, China) supplemented with 2% type IV collagenase (Cat. no. C5138-500MG, Sigma-Aldrich, United States) at 37 °C for 45 min. Next, the mixture was centrifuged at 1000 rpm for 6 min at 4 °C, and the cell pellets were resuspended in DMEM supplemented with 10% fetal bovine serum (FBS) (Cat. no. 10099158, Gibco, United States), which was replaced every 2-3 d, after which the cells were passaged at 90% confluence. The primary fibroblasts were used within passage 7 for all experiments, and at least 3 independent specimens were used for each experiment. Exos were isolated *via* ultracentrifugation at 120000 RCF for 18 h (overnight) (45Ti rotor, Beckman Coulter, United States), after which the supernatant was collected as exosome-free FBS[28]. DMEM supplemented with 10% Exo-free FBS or hucMSC-Exo was used to culture fibroblasts until they reached 60% confluence for subsequent functional experiments. All the incubations were performed at 37 °C with 5% CO₂.

Exo isolation, qualification and characterization

HucMSCs were purchased from Cyagen Company (Cat. no. HUXUC-01001, China) and expanded in basal medium (Cat. no. HUXUB-90011, Cyagen, China) supplemented with 10% FBS + culture supplement (for hucMSCs) (FBS for hucMSCs, Cat. no. HUXUB-05001, Cyagen, China) and 1% penicillin-streptomycin-amphotericin B agent (Cat. no. C125C8, New Cell & Molecular Biotech, China). HucMSCs between passages 3 and 6 were used for subsequent experiments. Exo-free FBS

Table 1 Clinical data of patients with and without pelvic organ prolapse

Parameters	Non-POP	POP	P value
Age (yr), mean ± SD	52.5 ± 7.184	57.9 ± 11.03	NS ¹
BMI (kg/m ²), mean ± SD	24.57 ± 3.655	23.3 ± 2.943	NS ¹
Parity (n), mean ± SD	1.8 ± 0.4216	1.2 ± 0.4206	NS ²
Menopause, n (%)	70%	50%	NS ³
POP stage, median (range)	0	3 (3-4)	< 0.0001

¹Independent sample *t* test.

²Welch's *t* test.

³Mann-Whitney test.

NS: Not significant; BMI: Body mass index; POP: Pelvic organ prolapse.

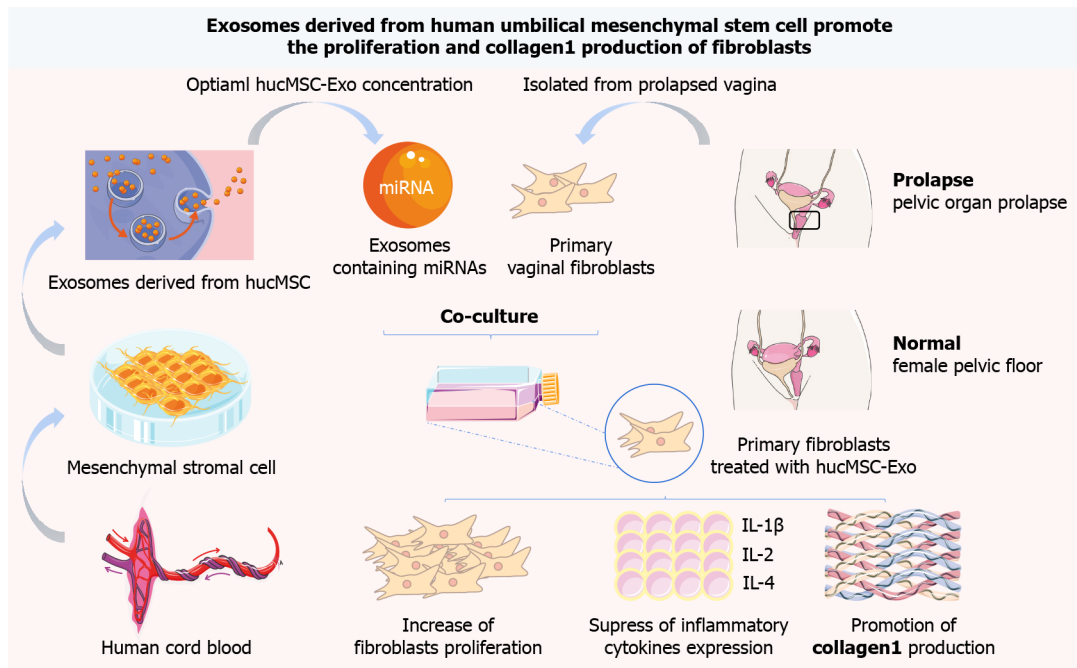


Figure 1 Human umbilical cord mesenchymal stromal cell-derived exosome promote the growth and collagen production of primary vaginal fibroblasts from patients with pelvic organ prolapse through microRNAs. hucMSC-Exo: Human umbilical cord mesenchymal stromal cell-derived exosome; miRNA: MicroRNA; hucMSCs: Human umbilical cord mesenchymal stromal cells; IL: Interleukin.

(10%; Cat. no. HUXUB-90012; Cyagen, China) was used when the hucMSCs reached 70% confluence. Forty-eight hours later, the conditioned medium was collected and processed according to the steps described in **Supplementary Figure 1C**. The collected Exos were stored in a -80 °C freezer for subsequent experiments.

Three methods were used to characterize the collected Exos. The morphology of the Exos was investigated by transmission electron microscopy (Tecnai G2 Spirit, FEI, United States). NanoSight tracking analysis (NTA) was used to determine the size distribution and concentration of the Exos with a NanoSight NS300 instrument (Malvern, United Kingdom). Western blotting was also used to assess Exo surface markers, including heat shock protein (HSP)70, TSG101 and CD81 (1:1000 dilution, Cat. no. ab275018, Abcam, Cambridge, United Kingdom).

Internalization of hucMSC-Exo by fibroblasts

The hucMSC-Exo were labeled with a PKH26 red fluorescence kit (MINI26, Sigma-Aldrich, United States). Then, 400 µg/mL Exos (40 µL) were resuspended in Diluent C solution (4 mL), and PKH26 ethanol dye solution (16 µL) was added to Diluent C (4 mL) to prepare a 2 × dye solution. After coincubation for 5 min and mixing every minute by pipetting, an equal volume of 10% Exo-depleted FBS was added to halt the staining. The labeled Exos were then ultracentrifuged at 100000 × g for 1 h and resuspended in DMEM supplemented with 10% Exo-free FBS (4 mL). The conditioned medium was incubated with fibroblasts at 37 °C for 12 h. The fibroblasts were washed with prechilled PBS, fixed with 4% PFA, and stained with F-actin (Cat. no. PF00001, Proteintech, China) and DAPI (Cat. no. P36935, Thermo, United States). The internalization of Exos by fibroblasts was observed with a fluorescence microscope (ECLIPSE E80i, Nikon, Tokyo, Japan) and a laser scanning confocal microscope (SP8, Leica, Germany).

Cell viability

A Cell Counting Kit-8 (CCK-8) (Cat. no. C6005; New Cell & Molecular Biotech, China) was used to examine the viability of primary vaginal fibroblasts. Fibroblasts were seeded in a 96-well plate (3×10^3 cells/well). After serum starvation for 12 h, the cells were treated with 4 or 6 $\mu\text{g}/\text{mL}$ hucMSC-Exo for 0 h, 24 h, 48 h or 72 h and then incubated with 10 μL of CCK-8 solution in 100 μL of fresh DMEM for 2 h. The optical density (OD₄₅₀) was measured by a microplate reader, and the results were analyzed manually using GraphPad Prism 9 (GraphPad Software 9.0, United States).

Gel contraction assay

The collected fibroblasts were digested with trypsin (Cat. no. C100C1; New Cell & Molecular Biotech, China), resuspended in culture medium and then mixed with prepared cold rat tail collagen type I (354236; Corning, United States), 1 N NaOH, 10 \times PBS and sterile dH₂O. The mixture was added to a 24-well plate with a volume of 500 μL and 1×10^5 cells in each well and then incubated at 37 °C and 5% CO₂ for 1 h. Next, 500 μL of 10% Exo-depleted medium containing certain Exos was added to each well. A sterile needle was used to release the gel after 48 h, and images were taken 4 h later. To determine the percent reduction in the gel area, images were taken with an ImageQuant™ LAS 4000 Luminescent Image Analyzer (GE Healthcare; Chicago, China) and analyzed with ImageJ software (National Institutes of Health, Bethesda, MA, United States).

Western blot analysis

After hucMSC-Exo treatment for 48 h, primary vaginal fibroblasts were lysed in RIPA lysis buffer containing 1% protease inhibitor (Cat. no. P002; New Cell & Molecular Biotech) after being washed twice with precooled PBS; then, the total protein concentration was determined *via* a bicinchoninic acid assay (Cat. no. ZJ102, epiZyme). All protein samples were separated *via* 10% sodium-dodecyl sulfate gel electrophoresis (Cat. no. PG212, epiZyme) and transferred to 0.22 μm polyvinylidene difluoride membranes (Cat. no. ISEQ00010, Millipore, United States); the membranes were blocked with 5% milk for 1 h and subsequently incubated with primary antibodies (Col1, 1:750, Servicebio, China) overnight at 4 °C. The next day, after being washed in Tris-buffered saline with Tween (TBST) 4 times for 8 min each, the membranes were incubated with an HRP-labeled secondary antibody (1:3000; Abcam, ab34710, United States) at room temperature for 1 h. Afterward, the membranes were washed with TBST 4 times for 8 min each, and the protein bands were detected on an ImageQuant™ LAS 4000 Luminescent Image Analyzer (GE Healthcare; Chicago, China). The data were analyzed by ImageJ for semiquantitative analysis.

Immunofluorescence

Fibroblasts (3×10^3 per well) were seeded on sterile coverslips in a 24-well plate and incubated with different concentrations of hucMSC-Exo (0, 4, or 6 $\mu\text{g}/\text{mL}$) for 48 h. The cells were washed with PBS three times and then fixed with 4% PFA for 15 min at room temperature. After being washed with PBS three additional times, the cells were treated with 0.1% Triton (Triton X-100; Cat. no. GC204003-100 mL; Servicebio, China) for 15 min and then blocked with goat serum for 1 h. Then, the cells were incubated with primary antibodies (1:500 dilution; Cat. no. ab34710; Abcam, United States) overnight at 4 °C. On the second day, the cells were incubated with secondary fluorescent antibodies (Cat. no. SA5-10150; Thermo Fisher Scientific, United States) and stained with DAPI. The stained cells were observed and photographed *via* Nikon fluorescence microscopy (Nikon, Tokyo, Japan).

Cell cycle analysis

Cell cycle analysis was performed to evaluate proliferative activity. Fibroblasts were seeded in a six-well plate (1×10^5 cells/well). After being cultured in serum-free medium for 12 h to ensure a synchronous cell cycle, the cells were exposed to 4 or 6 $\mu\text{g}/\text{mL}$ hucMSC-Exo for 48 h. Subsequently, the fibroblasts were collected and washed with prechilled PBS three times before propidium iodide staining (Cat. No. CCS012; MultiSciences, China) for 30 min at room temperature in the dark. The data were collected with a CytoFLEX (Beckman Coulter, United States) and analyzed with FlowJo 10 software (Ashland, OR, United States).

Total collagen synthesis assay

Primary vaginal fibroblasts reached 90% confluence after being cultured in hucMSC-Exo for 48 h, and the cell culture supernatant was collected. To determine the total secreted collagen content in the cell culture, which was generally lower than the standard range of Sirius Red detection, a concentrating solution (Cat. no. 90626, Chondrex, United States) was used first before the application of the Sirius Red Total Collagen Detection Assay Kit (Cat. no. 9062, Chondrex, United States). The colorimetric assay was performed according to the manufacturer's protocol. The absorbance was measured at 540 nm by a microplate reader. The collagen content in each group was calculated based on the collagen standard curve and is presented as the percentage of the collagen content in the control group.

Flow cytometry analysis of Col1 expression in fibroblasts

Cells (1×10^5 per well) were seeded in 6-well plates. After exposure to hucMSC-Exo for 48 h, the cells were harvested after treatment with trypsin/EDTA (Cat. no. C100C1, New Cell & Molecular Biotech, China) and washed twice with PBS. The cells were subsequently fixed with fix solution (Cat. no. G1101-500mL, Servicebio, China) and then stained with 1:50 diluted APC-conjugated anti-Col1 (Cat. no. 180610, Absin, China) for 30 min at 4 °C in the dark. The cells were then washed twice with Perm solution and suspended in staining buffer at a final volume of 300 μL . The data were acquired on a CytoFLEX system (Beckman Coulter, United States) and analyzed using FlowJo v10.4.

Enzyme-linked immunosorbent assay

Enzyme-linked immunosorbent assay (ELISA) kits (Cat. no. EH10268S, Cat. no. EH10270M, Cat. no. EH10291M, China) were used to quantify the expression of inflammatory cytokines [interleukin (IL)-1 β , IL-2 and IL-4] and transforming growth factor (TGF)- β 1 in the supernatants of cultured fibroblasts exposed to hucMSC-Exo. Briefly, the medium was collected and centrifuged at 400 \times g for 20 min to remove cell debris. The subsequent procedures were performed according to the manufacturer's protocols. The absorbance was measured at 450 nm. The results were analyzed with GraphPad Prism 9 (GraphPad Software, United States).

Quantitative real-time polymerase chain reaction analysis of gene expression in isolated primary fibroblasts

RNA extraction, cDNA synthesis and quantitative real-time polymerase chain reaction (RT-qPCR) were performed to assess the effect of hucMSC-Exo on the expression of genes related to the extracellular matrix (ECM) in fibroblasts. Briefly, total RNA was extracted from fibroblasts using an RNA purification kit (Cat. no. B0004DP, EZBioscience, United States), and a NanoDrop Spectrophotometer (Thermo Fisher Scientific) was used to determine the concentration of RNA. cDNA synthesis was subsequently performed using a reverse transcription kit (Cat. no. A0010CGQ, EZBioscience, United States) and mixtures of cDNA and SYBR Green qPCR master mix (Cat. no. A0012-R2, EZBioscience, United States) in a QuantStudio Flex Real-Time PCR System (Thermo Fisher Scientific, United States). GAPDH was used as a housekeeping gene for the normalization of expression, and the relative expression of the target genes was calculated by the $2^{-\Delta\Delta Ct}$ method. The sequences of the primers used in this study are shown in Table 2.

RNA-seq

Total RNA was extracted from POP and non-POP primary fibroblasts with TRIzol reagent (Cat. no. 15596026; Invitrogen, United States). A NanoDrop 2000 spectrophotometer (Thermo Scientific, United States) was used to assess RNA purity and to quantify RNA, and RNA integrity was assessed using an Agilent 2100 Bioanalyzer (Agilent Technologies, Santa Clara, United States). Then, libraries were constructed using the VAHTS Universal V6 RNA-seq Library Prep Kit in accordance with the manufacturer's instructions. Transcriptome sequencing and analysis were subsequently conducted by OE Biotech Co., Ltd. (Shanghai, China) and Genedenovo Biotechnology Co., Ltd. (Guangzhou, China). To ensure data quality, data filtering was performed on the raw data before information analysis. First, fastp was utilized for quality control of the raw reads generated from sequencing, filtering out low-quality data according to the criteria outlined below, to obtain clean reads[29]. The steps for read filtering included removing reads containing adapters, reads with a N ratio exceeding 10%, reads composed entirely of the A base and low-quality reads (bases with a Q-score \leq 20 constituting more than 50% of the entire read length). The quality distribution of bases and per-base sequence content were determined with filtered data. Then, sequencing randomness analysis was carried out for each sample.

mRNA sequencing analysis

The libraries were sequenced on an Illumina NovaSeq 6000 platform, and 150 bp paired-end reads were generated. The clean reads were subsequently mapped to the reference genome using HISAT2 2. The FPKM3 value for each gene was calculated, and the read counts for each gene were obtained from NCBI_GRCh38.p13. Differential expression analysis was performed using DESeq2[30]. A *P* value $<$ 0.05 and a fold change $<$ 15 were set as the thresholds for identifying significantly differentially expressed genes (DEGs). Hierarchical cluster analysis of DEGs was performed using R (v 3.2.0) to assess the expression patterns of genes in different groups and samples. Based on the hypergeometric distribution, Gene Ontology (GO)[31] and Reactome enrichment analyses of the DEGs were performed to screen for significantly enriched terms using R. Gene set enrichment analysis (GSEA) was performed using GSEA software[32,33].

miRNA sequencing

Total RNA was extracted from three replicate samples of hucMSC-Exo using the QubitTM microRNA Assay Kit (Q32880), and RNA integrity was assessed using a 2100 bioanalyzer (Agilent Technologies). An Illumina TruSeq Small RNA Kit (Illumina, San Diego, CA, United States) was used to construct a sequence library, and a high-throughput sequencing platform was used to sequence the enriched 18-32 nt small RNA fragments. Raw fastq-format data were first processed through in-house Perl scripts, and clean reads were obtained by removing reads containing adapters, poly-N sequences and sequences smaller than 15 nt or longer than 35 nt. The volume of sequencing data per sample fluctuated by no more than 10%, and bases detected with an accuracy of at least 99.9% (Q-score 30) accounted for more than 85%. The TargetScan, Ellmo, and Diana databases were used to predict the target genes of the miRNAs. GO enrichment analysis was also conducted for the identified target genes.

Statistical analysis

All the data were analyzed by GraphPad Prism 9.0 (GraphPad Software, Inc., United States) and are displayed as the mean \pm SD. All the experiments were performed independently at least three times. One-way analysis of variance (ANOVA) was used for comparisons among multiple groups (^a*P* $<$ 0.05; ^b*P* $<$ 0.01; ^c*P* $<$ 0.001; ^d*P* $<$ 0.0001).

Table 2 The primers sequences utilized in this study

Gene	Primer sequences
Col 1A1 FW	GTGCGATGACGTGATCTGTGA
Col 1A1 RV	CGGTGGTTTCTTGGTCGGT
Col 1A2 FW	TTGAAGGAGGATGTTCCCATCT
Col 1A2 RV	ACAGACACATATTTGGCATGGT
Col 3A1 FW	TTGAAGGAGGATGTTCCCATCT
Col 3A1 RV	ACAGACACATATTTGGCATGGT
MMP1 FW	CTCTGGAGTAATGTCACACCTCT
MMP1 RV	TGTTGGTCCACCTTTCATCTTC
TIMP1 FW	AGAGTGTCTGCGGATACTTCC
TIMP1 RV	CCAACAGGTAGGCTTGGTG
Elastin FW	GCAGGAGTTAAGCCCAAGG
Elastin RV	TGTAGGGCAGTCCATAGCCA
LOX FW	CGGCGGAGGAAAAGTGTCT
LOX RV	TCGGCTGGTAAGAAATCTGA
GAPDH FW	TGACATCAAGAAGGTGGTGAAGCAG
GAPDH RV	GTGTCGCTGTGAAGTCAGAGGAG

MMP1: Matrix metalloproteinase 1; TIMP1: Tissue inhibitor of matrix metalloprotease 1; LOX: Lysyl oxidase.

RESULTS

Disordered collagen fibers in the POP vaginal wall

Pathological examination was performed to identify abnormal collagen deposition in vaginal tissues collected from patients with and without POP by Masson and Sirius Red staining. Collagen was dyed blue by Masson’s trichrome stain and stained red by Sirius Red dye. Both Masson’s trichrome and Sirius Red staining *via* bright field microscopy revealed that the fibrotic area of the vaginal wall in the POP group was markedly smaller, more disorganized and looser than that in the control group (Figure 2A and B), which is consistent with the previous studies[2,4]. The qualification of collagen content in the vaginal wall determined by Masson’s trichrome and Sirius Red staining is shown in Figure 2C and D. In addition, to evaluate the collagen composition, Sirius Red-stained vaginal tissue was scanned by polarized light microscopy: Col1 is shown in red, and Col3 is shown in green. As shown in Figure 2E, there was a pronounced loss of Col1 in the POP group, an effect that was accompanied by irregular and thinner collagen bundles; in contrast, the collagen in the non-POP group was thicker, denser and more uniform. We subsequently evaluated the expression of Col1 *via* IHC and immunofluorescence (IF) (Figure 2F and G), and the results further confirmed that Col1 expression was notably decreased and that the structure was disrupted in POP-related vaginal tissues. Notably, primary fibroblasts in tissues from patients with POP are strongly involved in maintaining the integrity of the pelvic support system by regulating the catabolism and metabolism of collagen. The colocalization of vimentin with fibroblasts and Col1 was weaker in the POP-related abnormal pelvic environment than in the non-POP pelvic environment (Figure 2G). There was no signal in the secondary antibody-only control group, which excluded the possibility of nonspecific staining (Supplementary Figure 1A).

Differences in the gene expression profiles of human primary vaginal fibroblasts between the POP and non-POP groups

Fibroblasts from the vaginal wall are highly important for connective tissue, and alterations in fibroblast quantity and quality may contribute to the pathophysiology of POP and tissue regeneration after POP surgery[34]. And the tissue viability was evaluated *via* FCM (Supplementary Figure 1D and E). Given the importance of primary fibroblasts, we isolated these cells for *in vitro* experiments. First, human primary vaginal fibroblasts were identified by a typical spindle-shaped morphology (Figure 3B). And the expression of vimentin in the fibroblasts was assessed using IHC and IF (Figure 3A and C). Furthermore, the specific marker of α -smooth muscle actin and fibroblast specific protein-1 of fibroblasts were assessed by IF (Supplementary Figure 1B). To verify the differences in the gene expression profiles of human primary vaginal fibroblasts between patients with and without POP, RNA-seq was performed on fibroblasts from both groups of patients. In each sample, filtered data with a Q-score of at least 30 accounted for more than 93% (Supplementary Table 1), and a horizontal line in the base distribution indicated a balanced data composition (Supple-

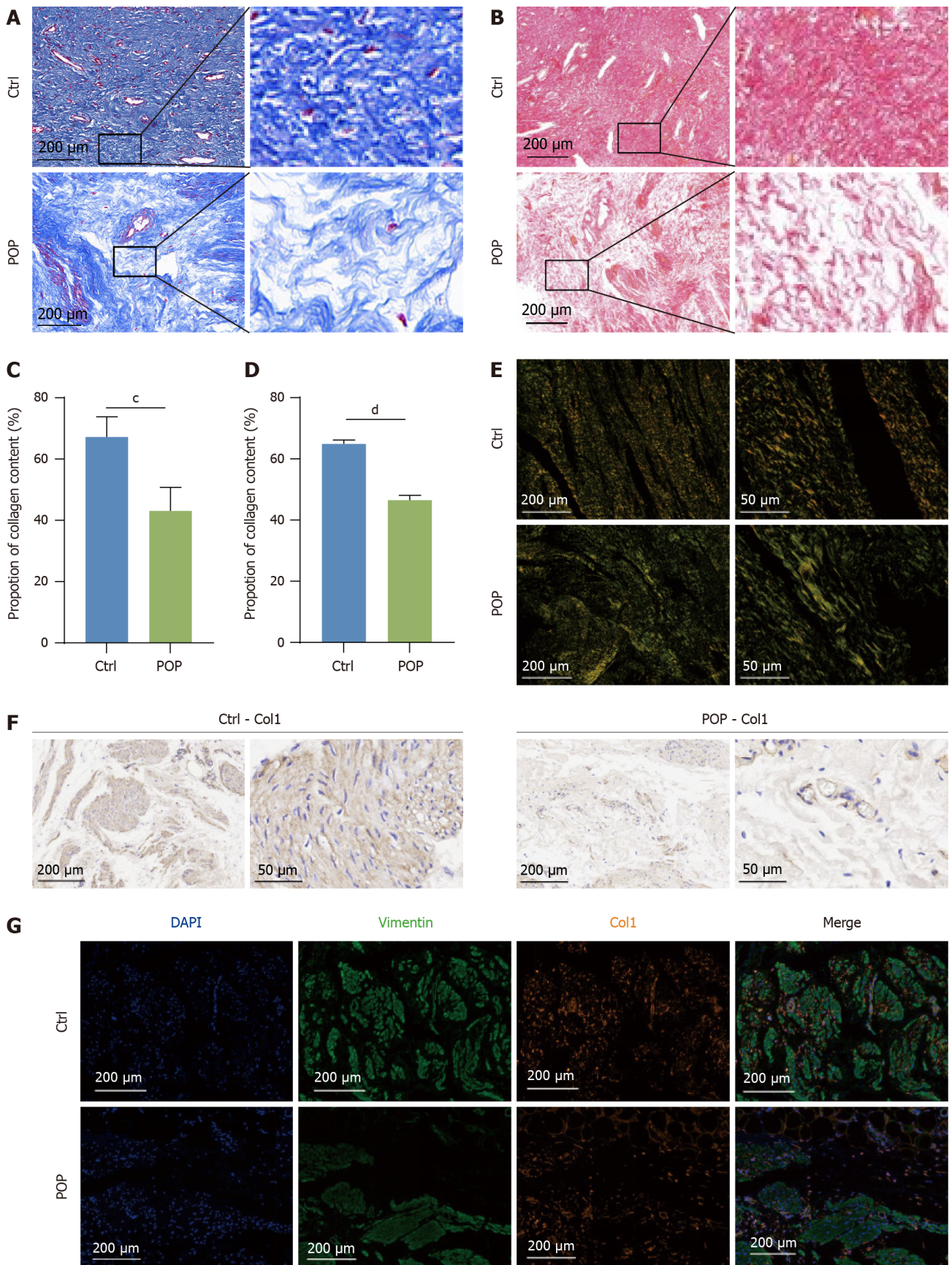


Figure 2 Differences in human vaginal collagen deposition between patients with and without pelvic organ prolapse. Disordered collagen fibers in the pelvic organ prolapse vaginal wall. A: Masson's trichrome staining images of vaginal tissues; B: Images of vaginal tissues stained with Sirius Red were collected by brightfield microscopy; C and D: Quantification of the collagen content in A and B; E: Sirius Red-stained tissues were scanned *via* polarized light microscopy; F: Representative immunohistochemistry images showing the distribution of Col1 in the human vaginal wall; G: Immunofluorescence showing the expression of Col1 and vimentin (a fibroblast marker) in the human vaginal wall. ^c*P* < 0.001; ^d*P* < 0.0001. POP: Pelvic organ prolapse.

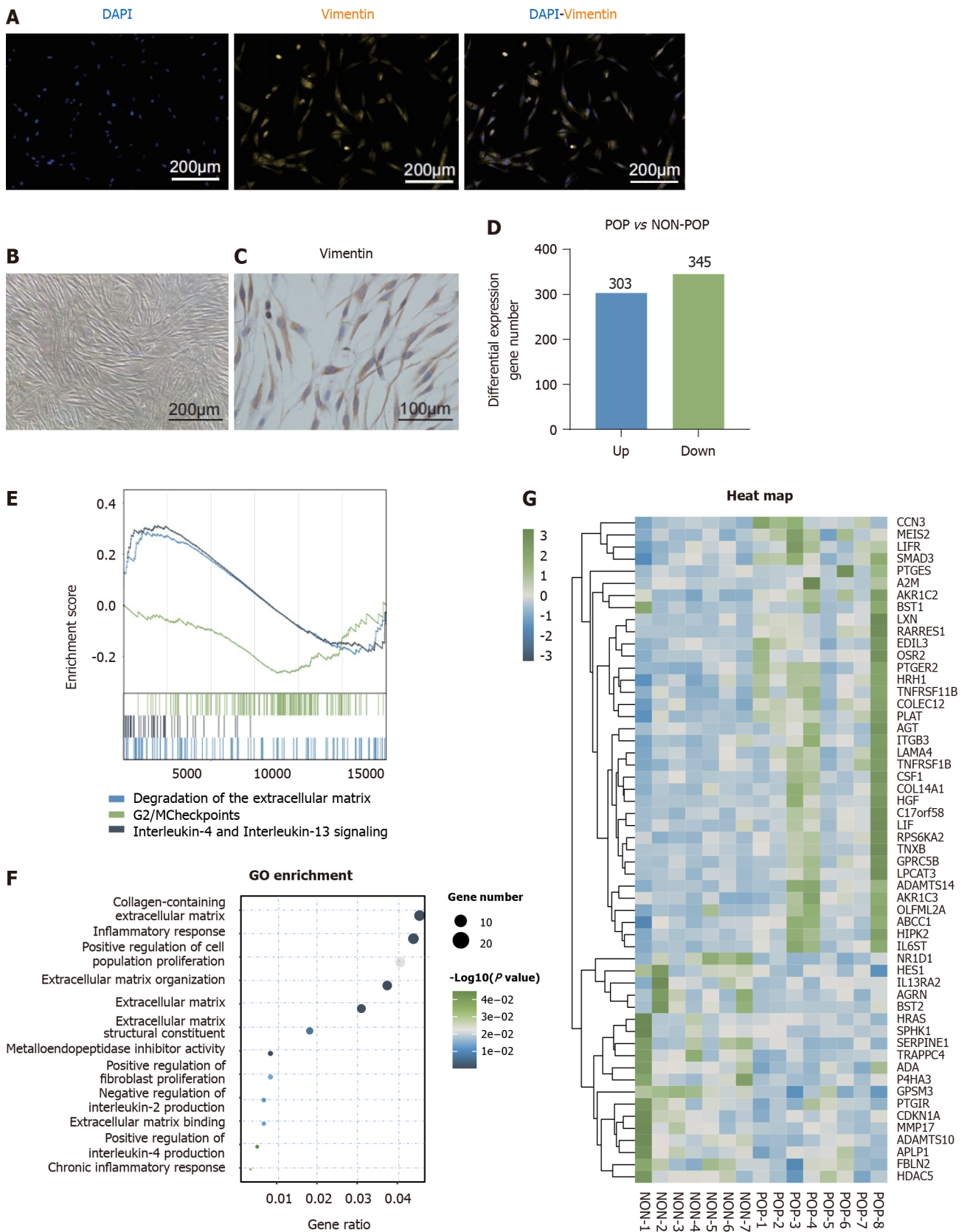


Figure 3 Differences in the gene expression profiles of human primary vaginal fibroblasts between the pelvic organ prolapse and non-pelvic organ prolapse groups. A: Images of primary vaginal fibroblasts for immunofluorescence; B: Images of primary vaginal fibroblasts for brightfield microscopy; C: Images of primary vaginal fibroblasts for immunohistochemistry; D: Number of differentially expressed genes (DEGs) between the pelvic organ prolapse (POP) and non-POP groups (fold change > 1.5, $P < 0.05$); E: Transcriptomic data were analyzed by Gene set enrichment analysis (false discovery rate > 0.25, $P < 0.05$); F: The above DEGs were further analyzed using Gene Ontology analysis ($P < 0.05$); G: Heatmaps were generated to show the DEGs of the two groups with respect to the previously mentioned terms. POP: Pelvic organ prolapse; GO: Gene Ontology.

mentary Figure 2A-O). Then sequencing randomness analysis of each sample was carried out, and the results revealed no apparent bias toward the 3' or 5' end (Supplementary Figure 3). All of these quality control checks suggested that the filtered data met the criteria. GSEA was used to compare the two groups to reveal functionally essential pathways involved in the occurrence and development of the disease; these pathways were related to the proliferation of cells, ECM remodeling and inflammatory processes, such as degradation of the ECM, G2_M checkpoints and IL-4 and IL-13 signaling (Figure 3E). According to DESeq software, a total of 648 DEGs were identified between the POP and non-POP groups, 303 of which were upregulated and 345 of which were downregulated (Figure 3D). Subsequently, GO enrichment analysis was performed on the DEGs, and the enriched functions were strongly related to cell proliferation, the ECM and inflammation (Figure 3F). A heatmap was generated to visualize the DEGs involved in these crucial processes (Figure 3G).

Exo identification and internalization

HucMSC-Exo were isolated and identified through TEM, NTA and western blotting, which were used to assess the morphology, size and surface marker expression of the Exos, respectively. TEM revealed that the hucMSC-Exo exhibited a cup-shaped morphology and obvious bilayer membrane structure (Figure 4A), and the particle size characteristically ranged between 80 and 200 nm (Figure 4B). Western blotting was used to confirm that the Exos were positive for appropriate surface markers, including HSP70, TSG101, and CD81 (Figure 4C). The above results showed that the Exos were extracted successfully. Subsequently, hucMSC-Exo labeled with PKH26 were incubated with fibroblasts whose cytoskeletons were then stained with F-actin-conjugated phalloidin. Fluorescence images demonstrated that hucMSC-Exo were internalized by fibroblasts (Figure 4D). The negative control group exhibited no red signal, which excluded nonspecific conjugation of PKH-26 dye and fibroblasts (Supplementary Figure 1F). Additionally, the 3D fluorescent image of hucMSC-Exo internalized by fibroblasts presented that red-labeled hucMSC-Exo was not colocalized with WGA-labeled cell membrane (Figure 4E). And the 3D videos of hucMSC-Exo internalization and the negative control group were shown in Videos 1 and 2. Efficiency of primary fibroblasts internalizing hucMSC-Exo within 24, 48, and 72 h were calculated with MFI *via* FCM which showed that hucMSC-Exo were internalized most at 48 h with 6 µg/mL (Figure 4F and G).

HucMSC-Exo stimulate the growth and contractility of fibroblasts

Previous research has confirmed reduced cellularity and impaired contraction in tissues from patients with POP[35]. To verify the effect of hucMSC-Exo on the function of fibroblasts, we performed a CCK-8 assay and cell cycle analysis to measure cell viability and proliferation, and contraction was assessed *via* a gel contraction assay.

The CCK-8 assay results showed that, compared to those of the other groups treated with excessively low or high concentrations of Exos, the viability of the fibroblasts treated with 4 or 6 µg/mL was substantially increased at 48 h. The effect of hucMSC-Exo on fibroblast viability was calculated as a percentage of that in the control group (Figure 5A and B). In addition, the cell cycle results were consistent with the CCK-8 assay results. Compared with those in the control group, the proportions of S- and G2-phase cells in the hucMSC-Exo groups were greater (Figure 5C and D). These results indicated that the cells exposed to hucMSC-Exo at an appropriate concentration were actively proliferating. Collagen gel contraction is a suitable *in vitro* model for revealing the cellular contraction process in tissue in three dimensions. When fibroblasts are cultured in a collagen gel, the gel contracts. As shown in Figure 5E and F, the collagen area in the groups treated with 4 and 6 µg/mL hucMSC-Exo for 48 h gradually decreased, suggesting that hucMSC-Exo promoted the contraction of fibroblasts in a dose-dependent manner. The expression of inflammatory cytokines (IL-1β, IL-2, and IL-4) was reduced in the Exo-treated group (Figure 5G-I), as determined *via* ELISAs. Taken together, these results demonstrated that hucMSC-Exo play a critical role in regulating the function of impaired fibroblasts from patients with POP.

HucMSC-Exo increase collagen production in primary vaginal fibroblasts

Col1 is an essential component of the ECM of connective tissues that is highly stretchable and resistant to tension. However, aged, disordered and decreased collagen fibrils are predominant in the pelvic tissue of patients with POP. To evaluate the expression of collagen in primary fibroblasts treated with UCMSC-Exo, multiple assays were carried out. First, Sirius Red dye was used to quantify the total collagen secreted into the fibroblast culture medium after treatment with hucMSC-Exo at different concentrations for 48 h. Fibroblasts exposed to hucMSC-Exo exhibited increased collagen in a dose-dependent manner (Figure 6A). TGF-β1 is regarded as a trigger of myofibroblast differentiation and ECM deposition[36]. Thus, we verified that the secretion of TGF-β1 from fibroblasts treated with hucMSC-Exo substantially increased after hucMSC-Exo stimulation for 48 h (Figure 6B). Furthermore, the impact of hucMSC-Exo on the expression of Col1 was measured by RT-qPCR (Figure 6C-E), flow cytometry (Figure 6F and H), IF (Figure 6G) and western blotting (Figure 6I), and the results were consistent with each other that the 6 µg/mL treatment had a greater capacity to stimulate the production of Col1, despite statistically significant differences were also observed between the 4 µg/mL treatment group and the control group (Figure 6F-I). For example, the median fluorescence intensity, mean gray value and Col1 expression were comparable in both the hucMSC-Exo-treated groups (4 and 6 µg/mL) and the control group; nonetheless, the group exposed to 6 µg/mL HucMSC-Exo had higher Col1 expression. In addition, Col1A1, Col1A2, and Col3A1 mRNA expression significantly differed between the fibroblasts treated with 6 µg/mL hucMSC-Exo and those from both the Exo-depleted group and the group treated with 10% FBS (the normal culture environment) (Figure 6C-E). Briefly, these results indicated that hucMSC-Exo regulated the expression of Col1 in primary vaginal fibroblasts.

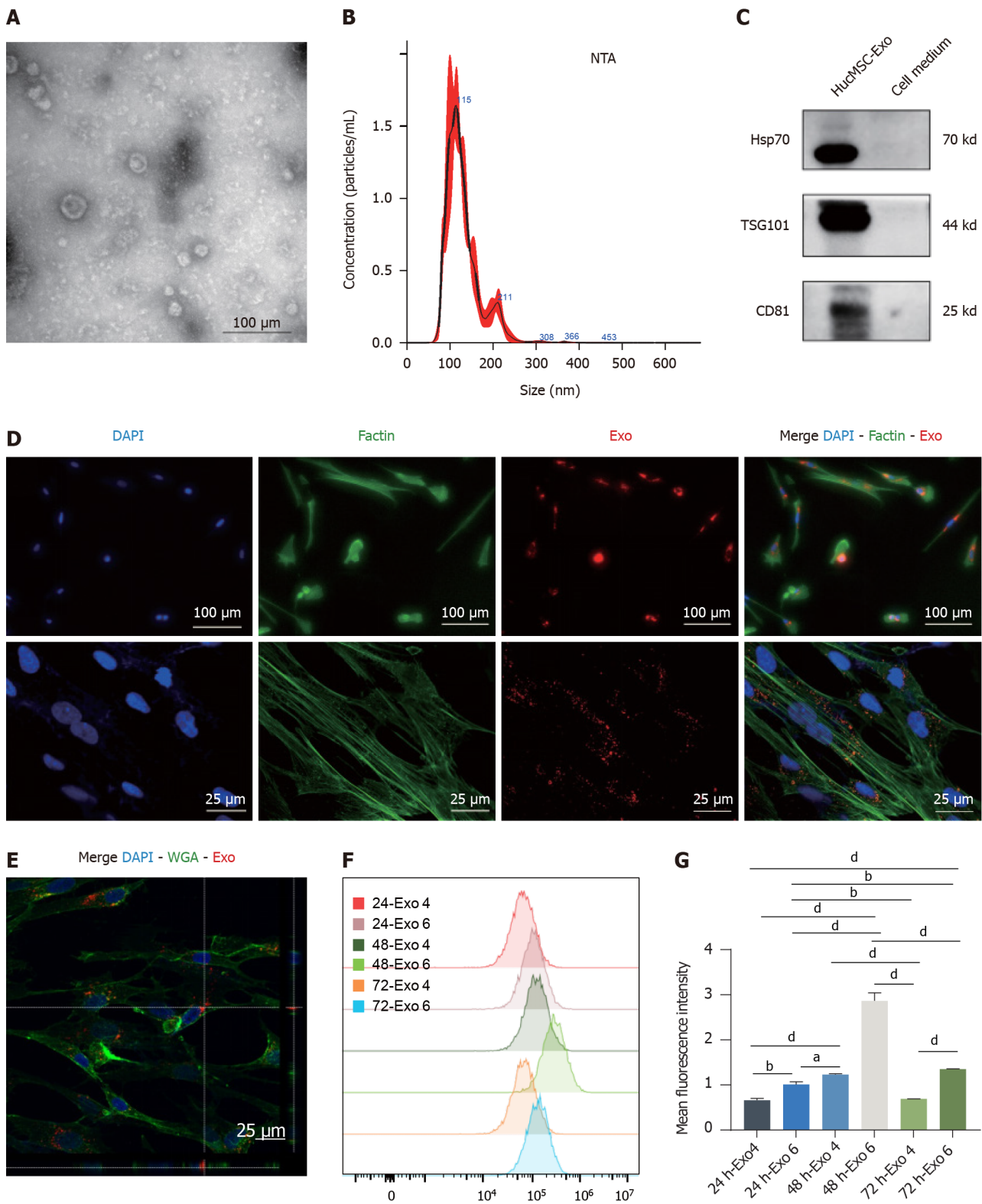


Figure 4 Identification and internalization of human umbilical cord mesenchymal stromal cell-derived exosomes. A: TEM was utilized to obtain representative images of human umbilical cord mesenchymal stromal cell-derived exosome (hucMSC-Exo) (scale bar: 200 μm); B: NTA of the size distribution and concentration of hucMSC-Exo; C: Western blot analysis for the detection of the hucMSC-Exo surface markers heat shock protein 70, TSG101, and CD81; D: Observation of PKH-26-hucMSC-Exo internalization by fibroblasts via both fluorescence microscopy and laser confocal microscopy; E: The 3D image of hucMSC-Exo internalized by fibroblasts; F and G: The median fluorescence intensity (F) and quantification (G) of hucMSC-Exo uptake by fibroblasts with 4 μg/mL and 6 μg/mL after treatment for 24, 48, and 72 h via FCM. DAPI is blue, PKH26 is red, F-actin is green in D, Wheat germ agglutinin is green in E. Scale bars: 50 μm and 25 μm. ^a*P* < 0.05; ^b*P* < 0.01; ^d*P* < 0.0001. HSP: Heat shock protein; Exo: Exosome.

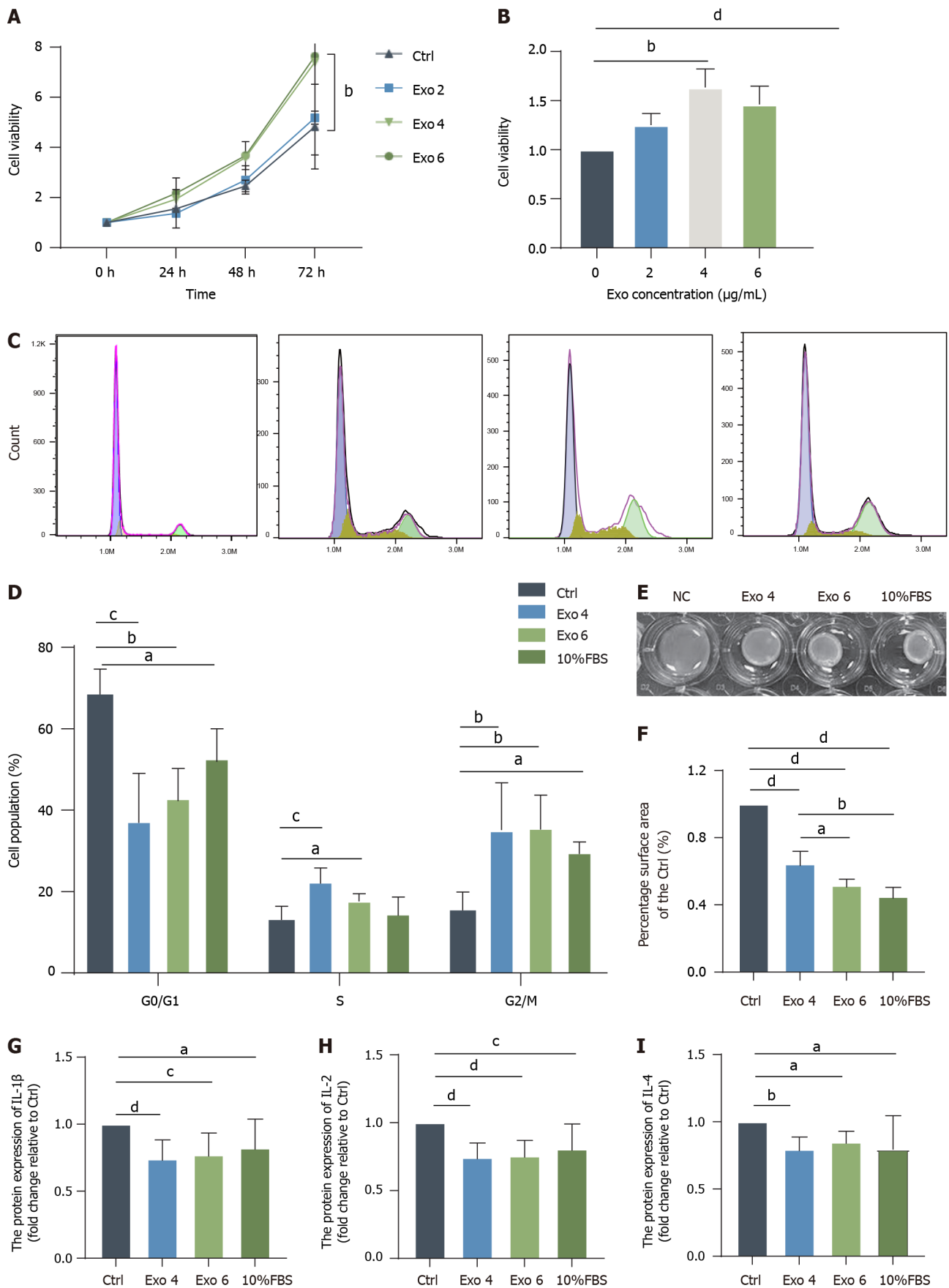


Figure 5 Human umbilical cord mesenchymal stromal cell-derived exosome stimulated the growth and contractility of fibroblasts. A: A Cell Counting Kit-8 (CCK-8) assay was used to detect the effect of human umbilical cord mesenchymal stromal cell-derived exosome (hucMSC-Exo) on the viability of fibroblasts from 0 h to 72 h; B: Quantification of the CCK-8 results at 48 h; C and D: Flow cytometric analysis of the cell cycle distribution of fibroblasts exposed to hucMSC-Exo and quantification of the results at 48 h; E and F: Representative images and quantification of gel contraction following incubation with hucMSC-Exo (4

or 6 µg/mL) for 48 h. Gel contraction was measured as a percentage of the area of the control group; G-I: Culture supernatant was collected after fibroblasts from the 4 groups were treated for 48 h, and enzyme-linked immunosorbent assay was conducted to determine the levels of interleukin (IL)-1β, IL-2 and IL-4. The data were analyzed by one-way ANOVA (means ± SD). ^aP < 0.05; ^bP < 0.01; ^cP < 0.001; ^dP < 0.0001. Exo: Exosome; IL: Interleukin; FBS: Fetal bovine serum.

HucMSC-Exo affect the gene expression profile of human primary vaginal fibroblasts

The mRNA expression levels of tissue inhibitor of metalloprotease 1 (TIMP1), MMP1, lysyl oxidase (LOX) and elastin were measured *via* RT-qPCR. Both groups exposed to hucMSC-Exo exhibited increased expression of TIMP1 (Figure 7A), while only fibroblasts treated with 6 µg/mL hucMSC-Exo exhibited decreased expression of MMP1 (Figure 7B). Elastin is another important component of the ECM, and LOX is responsible for the maturation of collagen and elastin and the crosslinking of collagens and elastin in the ECM. After treatment with 6 µg/mL hucMSC-Exo, the cells produced more elastin and LOX than did the control cells (Figure 7C and D). RNA was extracted from human primary vaginal fibroblasts from the control group and from fibroblasts exposed to hucMSC-Exo (4 or 6 µg/mL) for RNA-seq analysis to explore the underlying mechanisms by which hucMSC-Exo protect against the degeneration of fibroblasts in POP. The sequencing data quality preprocessing results are presented in Supplementary Table 2. The distribution of bases exhibits a horizontal line, which suggests qualified filtered data (Supplementary Figure 4A-O). The results of the randomness analysis for the filtered data suggested no apparent bias toward the 3' or 5' end (Supplementary Figure 5A-O). All these results guarantee the quality of the filtered data. Thus, further analysis was carried out with clean data. Pairwise Venn analysis revealed 203 overlapping DEGs between fibroblasts treated with 4 µg/mL and fibroblasts in the Exo-depleted group and between fibroblasts exposed to 6 µg/mL and fibroblasts in the Exo-depleted group (Figure 7E). Next, we focused on the above 203 DEGs, which are critical candidate genes involved in normalizing the function of impaired fibroblasts. These genes were subjected to bioinformatics analysis, including Reactome pathway analysis and GO analysis. As shown in Figure 7F, in the Reactome analysis, 8 biological processes were significantly enriched; these processes involved the regulation of inflammatory processes and, importantly, ECM remodeling, such as ECM organization, degeneration of the ECM and activation of MMPs. In addition, the GO analysis results suggested that hucMSC-Exo had regulatory effects on inflammatory processes and the ECM, findings that were consistent with the results of the Reactome analysis (Figure 7F). In addition, GO analysis indicated that hucMSC-Exo regulate proliferation, which is essential for fibroblasts; however, no differences were observed in the CCK-8 or cell cycle assay results (Figure 7G). Next, a Venn diagram was drawn to visualize the downregulated DEGs (Figure 7H). Moreover, a heatmap was constructed to show the mRNA expression of DEGs related to inflammatory processes and ECM organization (Figure 7I). Among the genes, MMP11 was expressed at lower levels in fibroblasts treated with hucMSCs and, according to the GO and Reactome analyses, was enriched in terms associated with the ECM.

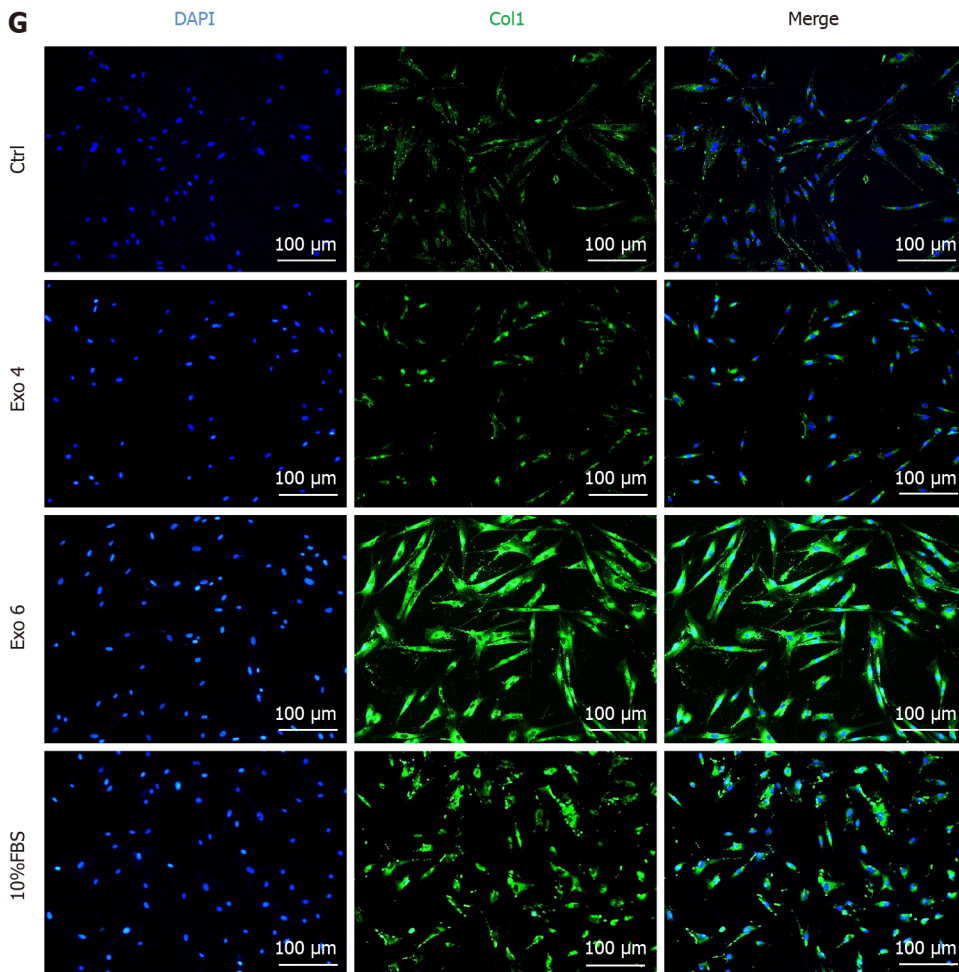
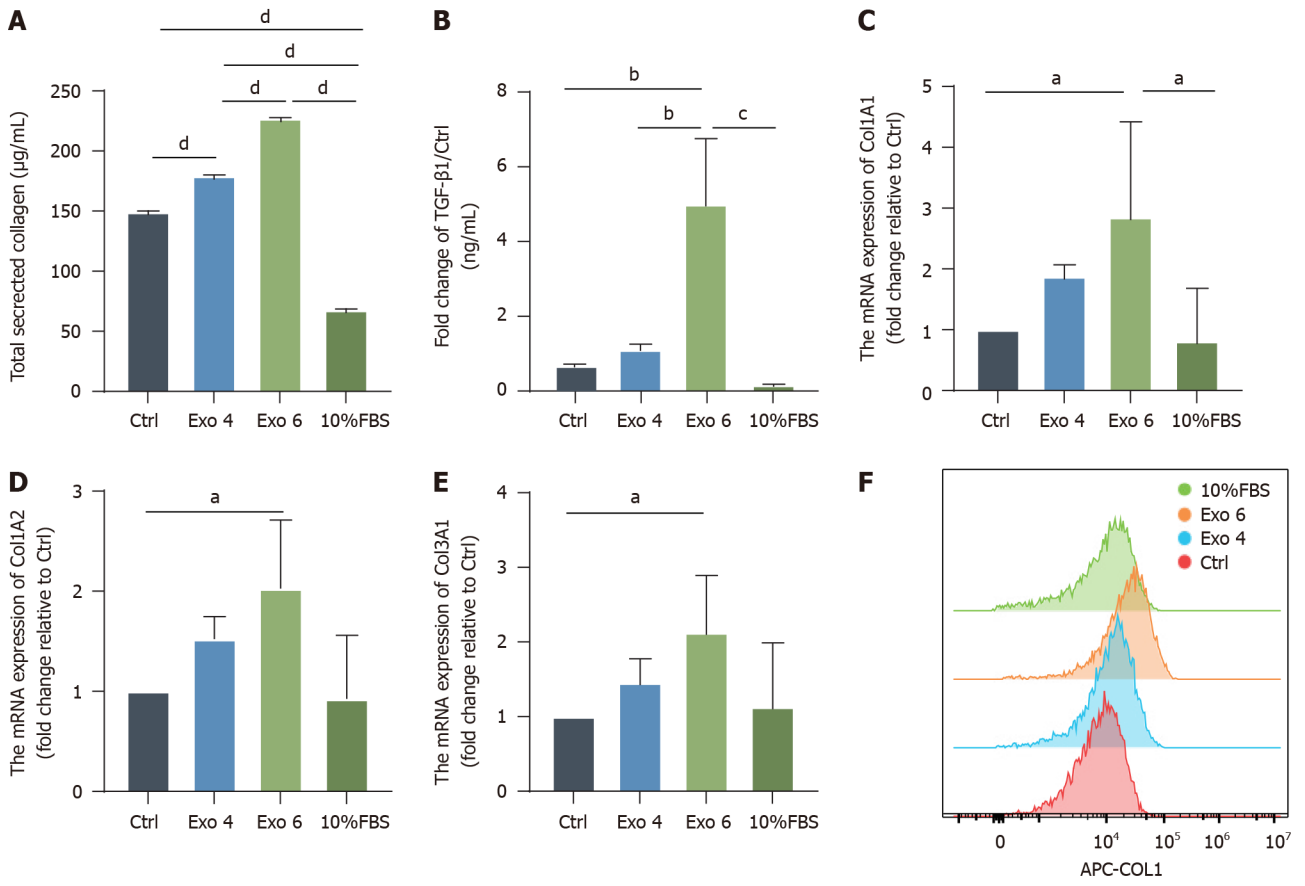
Characterization of miRNA profiles in hucMSC-Exo and identification of beneficial targeted miRNAs

The miRNAs carried by MSC-Exos are highly important and function as messengers to mediate cell-cell communication [37,38]. Consequently, miRNA sequencing of hucMSC-Exo further elucidated the mechanisms underlying their biological functions. The base calling errors are presented in Supplementary Figure 6 and Supplementary Table 3, which show the quality control of the raw data and the filtered data, which were used for further analysis. Firstly, our main aim was to identify the miRNAs that were expressed stably and at high abundance, which was defined by taking the intersection of the top 30 miRNAs from three hucMSC-Exo samples (Figure 8A) and the top 10 miRNAs, as depicted in Figure 8B. We subsequently focused on the downregulated DEGs in Exo-treated fibroblasts that were strongly correlated with the regulation of the ECM, identifying MMP11 as a candidate mRNA. Subsequently, three databases (TargetScan, Elmond, Diana) were utilized to predict the target miRNAs of MMP11 among the top 27 miRNAs in hucMSC-Exo. GO analysis was also conducted on the target miRNAs of the downregulated mRNA, MMP11, which showed that the miRNAs contained in hucMSC-Exo significantly promoted ECM remodeling (Figure 8C). Next, the RT-qPCR results indicated that fibroblasts had reduced MMP11 expression, which validated the previous RNA-seq results (Figure 8D).

DISCUSSION

The results of our study verified that the vaginal tissue of patients with POP displayed an abnormal collagen fiber distribution and that hucMSC-Exo promoted POP-related connective tissue repair. These findings demonstrated that hucMSC-Exo not only stimulated fibroblast growth by promoting cell viability and the cell cycle but also promoted the expression of Col1 *in vitro*. Herein, we clarified the therapeutic potential of hucMSC-Exo for POP fibroblasts, providing a prospective approach for treating POP.

POP is distinguished by the descent of pelvic organs into or out of the vagina and has a relatively high prevalence and recurrence rate[39,40]. This disorder results in severe discomfort, mental health issues and financial burdens on both individuals and society. Unfortunately, to date, treatments for POP involve physical and surgical methods, none of which achieve satisfactory curative effects. The application of transvaginal meshes in pelvic reconstruction surgery is prohibited due to the risk of severe complications. Recently, the application of stem cell-based therapy has attracted increased interest because of the powerful abilities of MSCs, such as self-renewal, multipotency and immunoregulation[41-43]. In addition, hucMSCs can be obtained in large quantities from medical waste and umbilical cord tissue, thus avoiding ethical issues. Moreover, Ma *et al*[15] reported that hucMSC transplantation can restore weak vaginal tissue by enhancing neovascularization and smooth muscle formation *in vivo*. Furthermore, our previous study showed that hucMSCs can



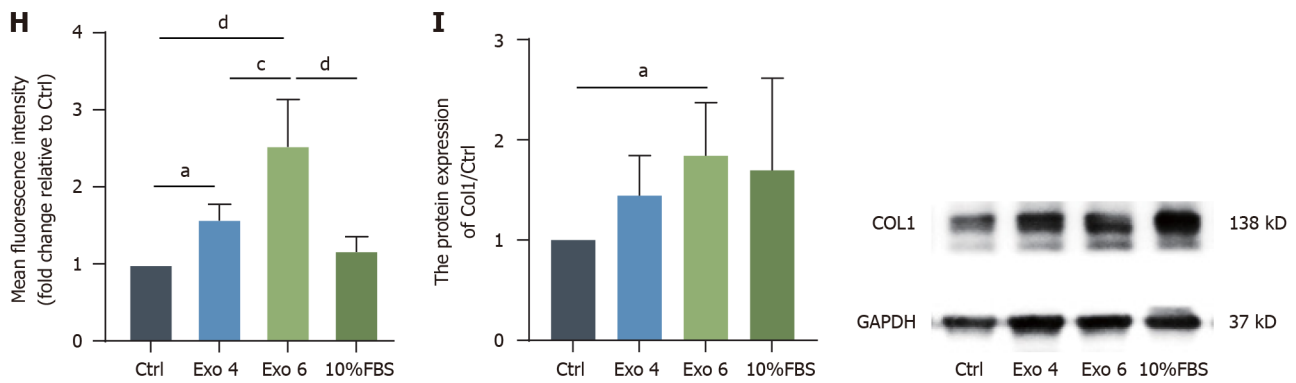


Figure 6 Human umbilical cord mesenchymal stromal cell-derived exosome promote the production of collagen in primary vaginal fibroblasts. A: A Sirius Red collagen staining kit was used to determine the total secreted collagen level in the fibroblasts' supernatant; B: Enzyme-linked immunosorbent assays were conducted to quantify the expression level of transforming growth factor- β 1 in the cell culture supernatant; C-E: Quantitative real-time polymerase chain reaction was performed to evaluate the mRNA levels of Col1A1, Col1A2 and Col3A1; F-H: Representative histogram overlay showing the median fluorescence intensity of each group (F) and quantification of these values (H), the expression level of Col1 was also detected by immunofluorescence. Green indicates Col1; blue indicates DAPI-stained nuclei. Scale bar: 100 μ m (G); I: The protein expression of Col1 was determined by western blot, and the results were quantified, which was in line with the previous results of Sirius Red staining, real-time polymerase chain reaction, FCM and immunofluorescence. The data are presented as the means \pm SEMs. Statistical analysis was performed with one-way ANOVA. ^a $P < 0.05$; ^b $P < 0.01$; ^c $P < 0.001$; ^d $P < 0.0001$. FBS: Fetal bovine serum; TGF: Transforming growth factor; Exo: Exosome.

inhibit the inflammatory response of human vaginal wall fibroblasts from patients with POP[19]. Thus, we selected hucMSCs from among other MSC sources.

Despite these considerable advantages of MSCs, their extensive application is limited by several notable factors, such as heterogeneity, potential tumorigenesis and thrombosis[16,17,44,45]. The therapeutic function of MSCs in tissue is dependent on their paracrine activity[46,47]. As one of the paracrine products of MSCs, Exos are potential candidates for medical application because of their safety and efficacy. Therefore, we aimed to isolate Exos from hucMSC culture media and hypothesized that hucMSC-Exo could be effective at restoring POP tissue.

Fibroblasts are predominantly responsible for remodeling POP connective tissue, which is mainly composed of collagen[48]. Col1 has a high stretching ability and resistance to tension. However, POP is characterized by a reduced quantity and impaired functionality of fibroblasts and collagen[1]. Surprisingly, our CCK-8 and cell cycle analysis results indicated that hucMSC-Exo increased cell viability and growth, consistent with the findings of previous studies[49]. Moreover, the expression of Col1 in fibroblasts increased after the application of hucMSC-Exo, as determined by western blotting, flow cytometry and IF *via* the use of a specific primary antibody against Col1. Collagen is a complex three-dimensional and highly dynamic structure. Thus, Sirius Red dye was utilized to assess the assembly of a collagen-specific site on three-dimensional structures because it can specifically bind to the [Gly-X-Y]_n helical structure on fibrillar collagen. We found that the total collagen secreted by fibroblasts treated with hucMSC-Exo was much greater than that secreted by fibroblasts in the control group.

The ECM in connective tissues is a highly dynamic structure that plays a critical role in the balance between MMPs and TIMPs. MMPs are zinc-dependent proteolytic enzymes that contribute to the remodeling of the ECM environment by cleaving ECM proteins[50,51]. MMP11, a member of the MMP family, is expressed transiently in mesenchymal cells and is associated with tissue remodeling[51,52]. POP tissue has been reported to have higher MMP and lower TIMP expression, indicating that the degradation of connective tissue exceeds its synthesis. Our results indicated that treatment with hucMSC-Exo increased the expression of TIMP1 and decreased the expression of MMP11 in primary fibroblasts.

miRNAs, which originate from stem-loop regions of longer RNA transcripts, are small regulatory RNAs of approximately 22 nt with a high degree of sequence conservation throughout evolution. The abundant miRNAs in MSC-derived Exos are highly important because they function as messengers to mediate cell-cell communication and subsequently regulate important biological processes by inducing target mRNA degradation and translational repression[38]. The highly expressed miRNAs in MSC-derived Exos are considered regulatory elements in the balance of the ECM[20,53,54].

Hence, we hypothesized that some of the top miRNAs expressed in hucMSC-Exo target MMP11 to promote collagen deposition in fibroblasts. Based on these findings, miRNA sequencing was carried out in hucMSC-Exo. Six of the top 17 enriched miRNAs in hucMSC-Exo were hsa-let-7a-5p, hsa-let-7c-5p, hsa-let-7e-5p, hsa-miR-29a-3p, hsa-let-7b-5p and hsa-miR-125a-5p, which all specifically targeted MMP11. As a result, we preliminarily speculated that hucMSC-Exo may play a critical role in the process of remodeling the ECM microenvironment by releasing miRNAs targeting MMP11. However, further studies are urgently needed to determine the impact of hucMSC-Exo *in vivo*. In addition, suitable Exo delivery methods should be developed in the future to improve the biocompatibility, cytotoxicity and degradation potential of these nanoparticles. In conclusion, we first demonstrated that hucMSC-Exo at certain concentrations facilitate fibroblast growth and ECM remodeling. These results suggested that hucMSC-Exo are a promising treatment for POP and may overcome current therapeutic difficulties.

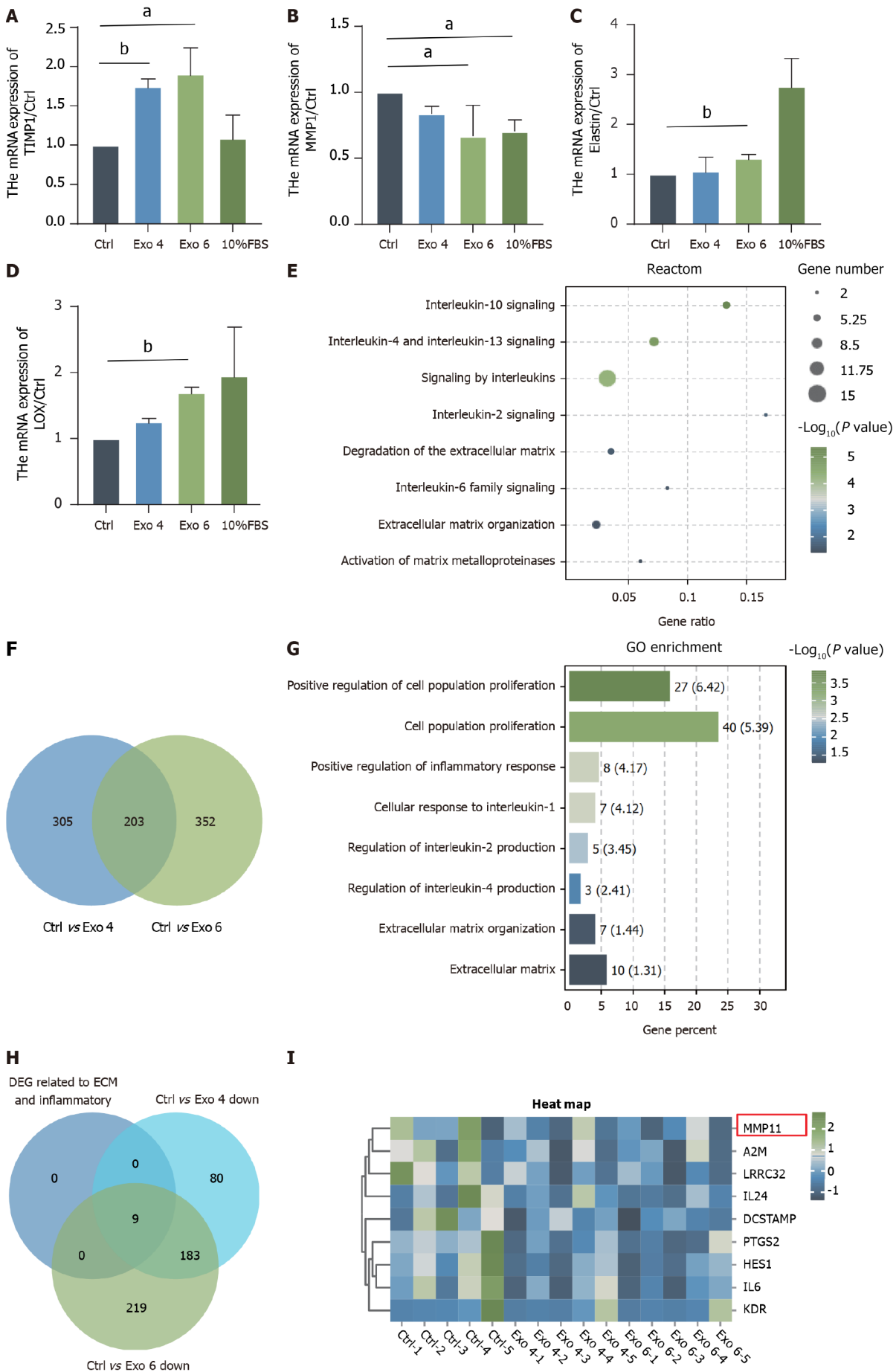


Figure 7 Effect of human umbilical cord mesenchymal stromal cell-derived exosome on the gene expression profile of human primary

vaginal fibroblasts. A-D: Quantitative real-time polymerase chain reaction was performed to evaluate the mRNA levels of tissue inhibitor of matrix metalloprotease 1, matrix metalloproteinase 1, elastin and lysyl oxidase; E: Venn diagrams were generated to show the shared differentially expressed genes (DEGs) from the comparison of the group treated with 4 $\mu\text{g/mL}$ versus the Exo-depleted group and the other group exposed to 4 $\mu\text{g/mL}$ versus the Exo-depleted group [fold change (FC) > 1.5, $P < 0.05$]. F and G: Reactome analysis (F) and Gene Ontology (G) analysis of the 203 overlapping genes; H: Venn diagrams showed DEGs about extracellular matrix (ECM) and inflammatory (FC > 1.5, $P < 0.05$); I: The heatmap depicting the 11 genes most related to inflammatory and ECM organization processes. ^a $P < 0.05$; ^b $P < 0.01$. TIMP1: Tissue inhibitor of matrix metalloprotease 1; MMP1: Matrix metalloproteinase 1; LOX: Lysyl oxidase; GO: Gene Ontology; FBS: Fetal bovine serum; Exo: Exosome.

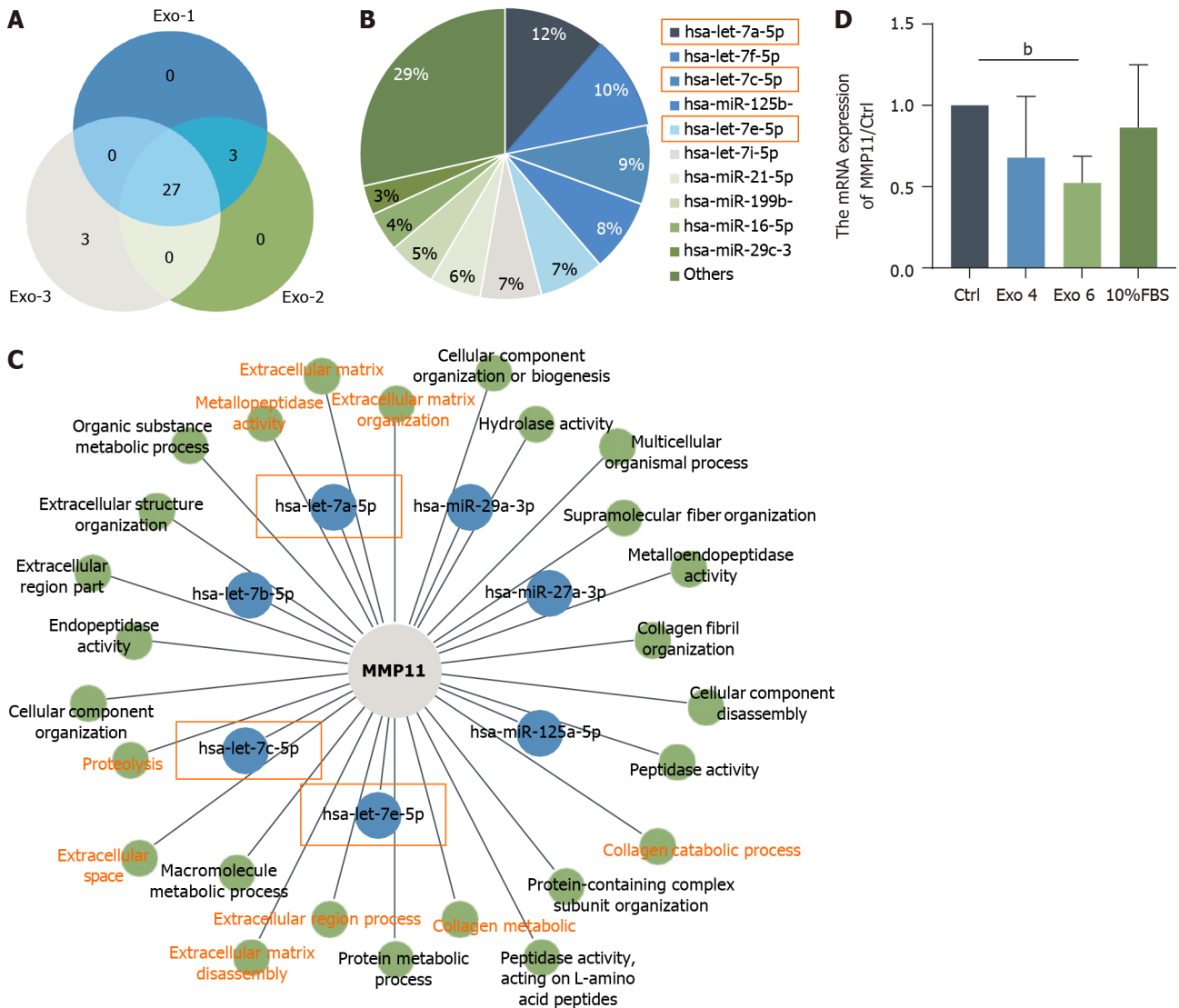


Figure 8 Characterization of microRNA profiles in human umbilical cord mesenchymal stromal cell-derived exosome and verification of beneficial targeted microRNAs. A: Venn diagram of the top 27 shared microRNAs (miRNAs) in human umbilical cord mesenchymal stromal cell-derived exosome (hucMSC-Exo) ($n = 3$); B: Pie charts showing the abundances of different miRNAs in hucMSC-Exo; C: The regulatory network depicting the predicted miRNAs of the gene of interest matrix metalloproteinase 11 (MMP11) in the top 27 list and the enrichment terms of these miRNAs in the Gene Ontology analysis; D: Quantitative real-time polymerase chain reaction was performed to evaluate the mRNA levels of MMP11. ^b $P < 0.01$. MMP: Matrix metalloproteinase; FBS: Fetal bovine serum; Exo: Exosome.

CONCLUSION

Our study demonstrated that hucMSC-Exo increased the growth and function of POP primary fibroblasts by increasing cell viability, the cell cycle, and the expression of Col1 *in vitro*. HucMSC-Exo-based therapy may be an ideal approach for treating POP safely and efficiently.

FOOTNOTES

Author contributions: Xu LM designed the study, performed the experiments, analyzed the data and wrote the manuscript; Yu XX and Chen YS edited the manuscript; Zhang N performed the experiments involved in revision stage; Chen YS interpreted the data; and all the authors read and approved the manuscript.

Supported by the National Natural Science Foundation of China, No. 81671439; the Science and Technology Commission of Shanghai Municipality, No. 21Y11906700 and No. 20Y11907300; and the Medical Innovation Research Project of the Science and Technology Commission of Shanghai Municipality, No. 22Y11906500.

Institutional review board statement: After approval from the Obstetrics and Gynecology Hospital of Fudan University (No. 2023-106), full-thickness biopsy specimens (0.5 cm²) from the vaginal wall were obtained from patients who underwent laparoscopic-assisted vaginal hysterectomy. Informed consent was obtained from all participants.

Conflict-of-interest statement: All the authors report no relevant conflicts of interest for this article.

Data sharing statement: The datasets analyzed during the current study are available from the corresponding author upon reasonable request.

Open-Access: This article is an open-access article that was selected by an in-house editor and fully peer-reviewed by external reviewers. It is distributed in accordance with the Creative Commons Attribution NonCommercial (CC BY-NC 4.0) license, which permits others to distribute, remix, adapt, build upon this work non-commercially, and license their derivative works on different terms, provided the original work is properly cited and the use is non-commercial. See: <https://creativecommons.org/licenses/by-nc/4.0/>

Country of origin: China

ORCID number: Yi-Song Chen [0000-0002-9234-8893](https://orcid.org/0000-0002-9234-8893).

S-Editor: Wang JJ

L-Editor: A

P-Editor: Yuan YY

REFERENCES

- Ruiz-Zapata AM**, Kerkhof MH, Zandieh-Doulabi B, Brölmann HA, Smit TH, Helder MN. Functional characteristics of vaginal fibroblastic cells from premenopausal women with pelvic organ prolapse. *Mol Hum Reprod* 2014; **20**: 1135-1143 [PMID: [25189765](https://pubmed.ncbi.nlm.nih.gov/25189765/) DOI: [10.1093/molehr/gau078](https://doi.org/10.1093/molehr/gau078)]
- Chen YS**, Hua KQ. Ultrastructure changes of uterosacral ligament and vaginal wall of patients with pelvic organ prolapse. *Shanghai Yixue* 2008; **490**: 2+533
- Zhu Y**, Li L, Xie T, Guo T, Zhu L, Sun Z. Mechanical stress influences the morphology and function of human uterosacral ligament fibroblasts and activates the p38 MAPK pathway. *Int Urogynecol J* 2022; **33**: 2203-2212 [PMID: [34036402](https://pubmed.ncbi.nlm.nih.gov/34036402/) DOI: [10.1007/s00192-021-04850-7](https://doi.org/10.1007/s00192-021-04850-7)]
- Zhu YP**, Xie T, Guo T, Sun ZJ, Zhu L, Lang JH. Evaluation of extracellular matrix protein expression and apoptosis in the uterosacral ligaments of patients with or without pelvic organ prolapse. *Int Urogynecol J* 2021; **32**: 2273-2281 [PMID: [32737532](https://pubmed.ncbi.nlm.nih.gov/32737532/) DOI: [10.1007/s00192-020-04446-7](https://doi.org/10.1007/s00192-020-04446-7)]
- Ruiz-Zapata AM**, Heinz A, Kerkhof MH, van de Westerlo-van Rijt C, Schmelzer CEH, Stoop R, Kluivers KB, Oosterwijk E. Extracellular Matrix Stiffness and Composition Regulate the Myofibroblast Differentiation of Vaginal Fibroblasts. *Int J Mol Sci* 2020; **21** [PMID: [32635512](https://pubmed.ncbi.nlm.nih.gov/32635512/) DOI: [10.3390/ijms21134762](https://doi.org/10.3390/ijms21134762)]
- Poncet S**, Meyer S, Richard C, Aubert JD, Juillerat-Jeanneret L. The expression and function of the endothelin system in contractile properties of vaginal myofibroblasts of women with uterovaginal prolapse. *Am J Obstet Gynecol* 2005; **192**: 426-432 [PMID: [15695982](https://pubmed.ncbi.nlm.nih.gov/15695982/) DOI: [10.1016/j.ajog.2004.09.018](https://doi.org/10.1016/j.ajog.2004.09.018)]
- Meyer S**, Achantari C, Hohlfeld P, Juillerat-Jeanneret L. The contractile properties of vaginal myofibroblasts: is the myofibroblasts contraction force test a valuable indication of future prolapse development? *Int Urogynecol J Pelvic Floor Dysfunct* 2008; **19**: 1399-1403 [PMID: [18511996](https://pubmed.ncbi.nlm.nih.gov/18511996/) DOI: [10.1007/s00192-008-0643-6](https://doi.org/10.1007/s00192-008-0643-6)]
- Fitz FF**, Resende AP, Stüpp L, Sartori MG, Girão MJ, Castro RA. Biofeedback for the treatment of female pelvic floor muscle dysfunction: a systematic review and meta-analysis. *Int Urogynecol J* 2012; **23**: 1495-1516 [PMID: [22426876](https://pubmed.ncbi.nlm.nih.gov/22426876/) DOI: [10.1007/s00192-012-1707-1](https://doi.org/10.1007/s00192-012-1707-1)]
- Alvarez J**, Cvach K, Dwyer P. Complications in pelvic floor surgery. *Minerva Ginecol* 2013; **65**: 53-67 [PMID: [23412020](https://pubmed.ncbi.nlm.nih.gov/23412020/)]
- Olsen AL**, Smith VJ, Bergstrom JO, Colling JC, Clark AL. Epidemiology of surgically managed pelvic organ prolapse and urinary incontinence. *Obstet Gynecol* 1997; **89**: 501-506 [PMID: [9083302](https://pubmed.ncbi.nlm.nih.gov/9083302/) DOI: [10.1016/s0029-7844\(97\)00058-6](https://doi.org/10.1016/s0029-7844(97)00058-6)]
- Farmer ZL**, Domínguez-Robles J, Mancinelli C, Larrañeta E, Lamprou DA. Urogynecological surgical mesh implants: New trends in materials, manufacturing and therapeutic approaches. *Int J Pharm* 2020; **585**: 119512 [PMID: [32526332](https://pubmed.ncbi.nlm.nih.gov/32526332/) DOI: [10.1016/j.ijpharm.2020.119512](https://doi.org/10.1016/j.ijpharm.2020.119512)]
- Mao M**, Li Y, Zhang Y, Kang J, Zhu L. Human umbilical cord mesenchymal stem cells reconstruct the vaginal wall of ovariectomized Sprague-Dawley rats: implications for pelvic floor reconstruction. *Cell Tissue Res* 2021; **386**: 571-583 [PMID: [34264376](https://pubmed.ncbi.nlm.nih.gov/34264376/) DOI: [10.1007/s00441-021-03478-9](https://doi.org/10.1007/s00441-021-03478-9)]
- Umer A**, Khan N, Greene DL, Habiba UE, Shamim S, Khayam AU. The Therapeutic Potential of Human Umbilical Cord Derived Mesenchymal Stem Cells for the Treatment of Premature Ovarian Failure. *Stem Cell Rev Rep* 2023; **19**: 651-666 [PMID: [36520408](https://pubmed.ncbi.nlm.nih.gov/36520408/) DOI: [10.1007/s12015-022-10493-y](https://doi.org/10.1007/s12015-022-10493-y)]

- 14 **Ahani-Nahayati M**, Niazi V, Moradi A, Pourjabbar B, Roozafzoon R, Keshel SH, Baradaran-Rafii A. Umbilical Cord Mesenchymal Stem/Stromal Cells Potential to Treat Organ Disorders; An Emerging Strategy. *Curr Stem Cell Res Ther* 2022; **17**: 126-146 [PMID: 34493190 DOI: 10.2174/1574888X16666210907164046]
- 15 **Ma Y**, Zhang Y, Chen J, Li L, Liu X, Zhang L, Ma C, Wang Y, Tian W, Song X, Li Y, Zhu L. Mesenchymal stem cell-based bioengineered constructs enhance vaginal repair in ovariectomized rhesus monkeys. *Biomaterials* 2021; **275**: 120863 [PMID: 34139509 DOI: 10.1016/j.biomaterials.2021.120863]
- 16 **Li JJ**, Hosseini-Beheshti E, Grau GE, Zreiqat H, Little CB. Stem Cell-Derived Extracellular Vesicles for Treating Joint Injury and Osteoarthritis. *Nanomaterials (Basel)* 2019; **9** [PMID: 30769853 DOI: 10.3390/nano9020261]
- 17 **Ribeiro-Rodrigues TM**, Laundos TL, Pereira-Carvalho R, Batista-Almeida D, Pereira R, Coelho-Santos V, Silva AP, Fernandes R, Zuzarte M, Enguita FJ, Costa MC, Pinto-do-Ó P, Pinto MT, Gouveia P, Ferreira L, Mason JC, Pereira P, Kwak BR, Nascimento DS, Girão H. Exosomes secreted by cardiomyocytes subjected to ischaemia promote cardiac angiogenesis. *Cardiovasc Res* 2017; **113**: 1338-1350 [PMID: 28859292 DOI: 10.1093/cvr/cvx118]
- 18 **Borgovan T**, Crawford L, Nwizu C, Quesenberry P. Stem cells and extracellular vesicles: biological regulators of physiology and disease. *Am J Physiol Cell Physiol* 2019; **317**: C155-C166 [PMID: 30917031 DOI: 10.1152/ajpcell.00017.2019]
- 19 **Li L**, Sima Y, Wang Y, Zhou J, Wang L, Chen Y. The cytotoxicity of advanced glycation end products was attenuated by UCMSCs in human vaginal wall fibroblasts by inhibition of an inflammatory response and activation of PI3K/AKT/PTEN. *Biosci Trends* 2020; **14**: 263-270 [PMID: 32493859 DOI: 10.5582/bst.2020.03125]
- 20 **Bian D**, Wu Y, Song G, Azizi R, Zamani A. The application of mesenchymal stromal cells (MSCs) and their derivative exosome in skin wound healing: a comprehensive review. *Stem Cell Res Ther* 2022; **13**: 24 [PMID: 35073970 DOI: 10.1186/s13287-021-02697-9]
- 21 **Jun EK**, Zhang Q, Yoon BS, Moon JH, Lee G, Park G, Kang PJ, Lee JH, Kim A, You S. Hypoxic conditioned medium from human amniotic fluid-derived mesenchymal stem cells accelerates skin wound healing through TGF- β /SMAD2 and PI3K/Akt pathways. *Int J Mol Sci* 2014; **15**: 605-628 [PMID: 24398984 DOI: 10.3390/ijms15010605]
- 22 **Shi Y**, Shu B, Yang R, Xu Y, Xing B, Liu J, Chen L, Qi S, Liu X, Wang P, Tang J, Xie J. Wnt and Notch signaling pathway involved in wound healing by targeting c-Myc and Hes1 separately. *Stem Cell Res Ther* 2015; **6**: 120 [PMID: 26076648 DOI: 10.1186/s13287-015-0103-4]
- 23 **Neybecker P**, Henrionnet C, Pape E, Mainard D, Galois L, Loeuille D, Gillet P, Pinzano A. *In vitro* and *in vivo* potentialities for cartilage repair from human advanced knee osteoarthritis synovial fluid-derived mesenchymal stem cells. *Stem Cell Res Ther* 2018; **9**: 329 [PMID: 30486903 DOI: 10.1186/s13287-018-1071-2]
- 24 **Wang AT**, Zhang QF, Wang NX, Yu CY, Liu RM, Luo Y, Zhao YJ, Xiao JH. Cocktail of Hyaluronic Acid and Human Amniotic Mesenchymal Cells Effectively Repairs Cartilage Injuries in Sodium Iodoacetate-Induced Osteoarthritis Rats. *Front Bioeng Biotechnol* 2020; **8**: 87 [PMID: 32211385 DOI: 10.3389/fbioe.2020.00087]
- 25 **Valadi H**, Ekström K, Bossios A, Sjöstrand M, Lee JJ, Lötvall JO. Exosome-mediated transfer of mRNAs and microRNAs is a novel mechanism of genetic exchange between cells. *Nat Cell Biol* 2007; **9**: 654-659 [PMID: 17486113 DOI: 10.1038/ncb1596]
- 26 **Bump RC**, Mattiasson A, Bø K, Brubaker LP, DeLancey JO, Klarskov P, Shull BL, Smith AR. The standardization of terminology of female pelvic organ prolapse and pelvic floor dysfunction. *Am J Obstet Gynecol* 1996; **175**: 10-17 [PMID: 8694033 DOI: 10.1016/s0002-9378(96)70243-0]
- 27 **Sima Y**, Li J, Xu L, Xiao C, Li L, Wang L, Chen Y. Quercetin antagonized advanced glycated end products induced apoptosis and functional inhibition of fibroblasts from the prolapsed uterosacral ligament. *Drug Discov Ther* 2024; **17**: 415-427 [PMID: 38044121 DOI: 10.5582/ddt.2023.01047]
- 28 **Shelke GV**, Lässer C, Gho YS, Lötvall J. Importance of exosome depletion protocols to eliminate functional and RNA-containing extracellular vesicles from fetal bovine serum. *J Extracell Vesicles* 2014; **3** [PMID: 25317276 DOI: 10.3402/jev.v3.24783]
- 29 **Chen S**, Zhou Y, Chen Y, Gu J. fastp: an ultra-fast all-in-one FASTQ preprocessor. *Bioinformatics* 2018; **34**: i884-i890 [PMID: 30423086 DOI: 10.1093/bioinformatics/bty560]
- 30 **Love MI**, Huber W, Anders S. Moderated estimation of fold change and dispersion for RNA-seq data with DESeq2. *Genome Biol* 2014; **15**: 550 [PMID: 25516281 DOI: 10.1186/s13059-014-0550-8]
- 31 **The Gene Ontology Consortium**. The Gene Ontology Resource: 20 years and still GOing strong. *Nucleic Acids Res* 2019; **47**: D330-D338 [PMID: 30395331 DOI: 10.1093/nar/gky1055]
- 32 **Subramanian A**, Tamayo P, Mootha VK, Mukherjee S, Ebert BL, Gillette MA, Paulovich A, Pomeroy SL, Golub TR, Lander ES, Mesirov JP. Gene set enrichment analysis: a knowledge-based approach for interpreting genome-wide expression profiles. *Proc Natl Acad Sci U S A* 2005; **102**: 15545-15550 [PMID: 16199517 DOI: 10.1073/pnas.0506580102]
- 33 **Mootha VK**, Lindgren CM, Eriksson KF, Subramanian A, Sihag S, Lehar J, Puigserver P, Carlsson E, Ridderstråle M, Laurila E, Houstis N, Daly MJ, Patterson N, Mesirov JP, Golub TR, Tamayo P, Spiegelman B, Lander ES, Hirschhorn JN, Altshuler D, Groop LC. PGC-1 α -responsive genes involved in oxidative phosphorylation are coordinately downregulated in human diabetes. *Nat Genet* 2003; **34**: 267-273 [PMID: 12808457 DOI: 10.1038/ng1180]
- 34 **Guler Z**, Roovers JP. Role of Fibroblasts and Myofibroblasts on the Pathogenesis and Treatment of Pelvic Organ Prolapse. *Biomolecules* 2022; **12** [PMID: 35053242 DOI: 10.3390/biom12010094]
- 35 **Takacs P**, Nassiri M, Gualtieri M, Candiotti K, Medina CA. Uterosacral ligament smooth muscle cell apoptosis is increased in women with uterine prolapse. *Reprod Sci* 2009; **16**: 447-452 [PMID: 19092052 DOI: 10.1177/1933719108328611]
- 36 **Ding H**, Chen J, Qin J, Chen R, Yi Z. TGF- β -induced α -SMA expression is mediated by C/EBP β acetylation in human alveolar epithelial cells. *Mol Med* 2021; **27**: 22 [PMID: 33663392 DOI: 10.1186/s10020-021-00283-6]
- 37 **Wu L**, Tian X, Zuo H, Zheng W, Li X, Yuan M, Tian X, Song H. miR-124-3p delivered by exosomes from heme oxygenase-1 modified bone marrow mesenchymal stem cells inhibits ferroptosis to attenuate ischemia-reperfusion injury in steatotic grafts. *J Nanobiotechnology* 2022; **20**: 196 [PMID: 35459211 DOI: 10.1186/s12951-022-01407-8]
- 38 **O'Brien J**, Hayder H, Zayed Y, Peng C. Overview of MicroRNA Biogenesis, Mechanisms of Actions, and Circulation. *Front Endocrinol (Lausanne)* 2018; **9**: 402 [PMID: 30123182 DOI: 10.3389/fendo.2018.00402]
- 39 **Sun B**, Zhou L, Wen Y, Wang C, Baer TM, Pera RR, Chen B. Proliferative behavior of vaginal fibroblasts from women with pelvic organ prolapse. *Eur J Obstet Gynecol Reprod Biol* 2014; **183**: 1-4 [PMID: 25461341 DOI: 10.1016/j.ejogrb.2014.09.040]
- 40 **Wu X**, Jia Y, Sun X, Wang J. Acceleration of pelvic tissue generation by overexpression of basic fibroblast growth factor in stem cells. *Connect Tissue Res* 2022; **63**: 256-268 [PMID: 33627007 DOI: 10.1080/03008207.2021.1895130]

- 41 **Karimineko S**, Movassaghpour A, Rahimzadeh A, Talebi M, Shamsasenjan K, Akbarzadeh A. Implications of mesenchymal stem cells in regenerative medicine. *Artif Cells Nanomed Biotechnol* 2016; **44**: 749-757 [PMID: 26757594 DOI: 10.3109/21691401.2015.1129620]
- 42 **Cheng J**, Zhao ZW, Wen JR, Wang L, Huang LW, Yang YL, Zhao FN, Xiao JY, Fang F, Wu J, Miao YL. Status, challenges, and future prospects of stem cell therapy in pelvic floor disorders. *World J Clin Cases* 2020; **8**: 1400-1413 [PMID: 32368533 DOI: 10.12998/wjcc.v8.i8.1400]
- 43 **Hassan WU**, Greiser U, Wang W. Role of adipose-derived stem cells in wound healing. *Wound Repair Regen* 2014; **22**: 313-325 [PMID: 24844331 DOI: 10.1111/wrr.12173]
- 44 **Bowers DT**, Brown JL. Nanofiber curvature with Rho GTPase activity increases mouse embryonic fibroblast random migration velocity. *Integr Biol (Camb)* 2021; **13**: 295-308 [PMID: 35022716 DOI: 10.1093/intbio/zyab022]
- 45 **Wang LT**, Liu KJ, Sytwu HK, Yen ML, Yen BL. Advances in mesenchymal stem cell therapy for immune and inflammatory diseases: Use of cell-free products and human pluripotent stem cell-derived mesenchymal stem cells. *Stem Cells Transl Med* 2021; **10**: 1288-1303 [PMID: 34008922 DOI: 10.1002/sctm.21-0021]
- 46 **Huang B**, Lu J, Ding C, Zou Q, Wang W, Li H. Exosomes derived from human adipose mesenchymal stem cells improve ovary function of premature ovarian insufficiency by targeting SMAD. *Stem Cell Res Ther* 2018; **9**: 216 [PMID: 30092819 DOI: 10.1186/s13287-018-0953-7]
- 47 **Wu P**, Zhang B, Shi H, Qian H, Xu W. MSC-exosome: A novel cell-free therapy for cutaneous regeneration. *Cytotherapy* 2018; **20**: 291-301 [PMID: 29434006 DOI: 10.1016/j.jcyt.2017.11.002]
- 48 **Li Y**, Nie N, Gong L, Bao F, An C, Cai H, Yao X, Liu Y, Yang C, Wu B, Zou X. Structural, functional and molecular pathogenesis of pelvic organ prolapse in patient and Lox11 deficient mice. *Aging (Albany NY)* 2021; **13**: 25886-25902 [PMID: 34923484 DOI: 10.18632/aging.203777]
- 49 **Zhu Z**, Zhang Y, Zhang Y, Zhang H, Liu W, Zhang N, Zhang X, Zhou G, Wu L, Hua K, Ding J. Exosomes derived from human umbilical cord mesenchymal stem cells accelerate growth of VK2 vaginal epithelial cells through MicroRNAs *in vitro*. *Hum Reprod* 2019; **34**: 248-260 [PMID: 30576496 DOI: 10.1093/humrep/dey344]
- 50 **Tan B**, Jaulin A, Bund C, Outilaft H, Wendling C, Chenard MP, Alpy F, Cicek AE, Namer IJ, Tomasetto C, Dali-Youcef N. Matrix Metalloproteinase-11 Promotes Early Mouse Mammary Gland Tumor Growth through Metabolic Reprogramming and Increased IGF1/AKT/FoxO1 Signaling Pathway, Enhanced ER Stress and Alteration in Mitochondrial UPR. *Cancers (Basel)* 2020; **12** [PMID: 32825455 DOI: 10.3390/cancers12092357]
- 51 **Alcantara MC**, Suzuki K, Acebedo AR, Kajioka D, Hirohata S, Kaisho T, Hatano Y, Yamagata K, Takahashi S, Yamada G. Androgen-regulated MafB drives cell migration *via* MMP11-dependent extracellular matrix remodeling in mice. *iScience* 2022; **25**: 105609 [PMID: 36465133 DOI: 10.1016/j.isci.2022.105609]
- 52 **Lefebvre O**, Wolf C, Limacher JM, Hutin P, Wendling C, LeMeur M, Basset P, Rio MC. The breast cancer-associated stromelysin-3 gene is expressed during mouse mammary gland apoptosis. *J Cell Biol* 1992; **119**: 997-1002 [PMID: 1429845 DOI: 10.1083/jcb.119.4.997]
- 53 **Ju Y**, Hu Y, Yang P, Xie X, Fang B. Extracellular vesicle-loaded hydrogels for tissue repair and regeneration. *Mater Today Bio* 2023; **18**: 100522 [PMID: 36593913 DOI: 10.1016/j.mtbio.2022.100522]
- 54 **Tang Q**, Lu B, He J, Chen X, Fu Q, Han H, Luo C, Yin H, Qin Z, Lyu D, Zhang L, Zhou M, Yao K. Exosomes-loaded thermosensitive hydrogels for corneal epithelium and stroma regeneration. *Biomaterials* 2022; **280**: 121320 [PMID: 34923312 DOI: 10.1016/j.biomaterials.2021.121320]



Published by **Baishideng Publishing Group Inc**
7041 Koll Center Parkway, Suite 160, Pleasanton, CA 94566, USA
Telephone: +1-925-3991568
E-mail: office@baishideng.com
Help Desk: <https://www.f6publishing.com/helpdesk>
<https://www.wjgnet.com>

